ASSESSING THE POTENTIAL OF SULFUR ISOTOPES AND TRACE METALS AS CHEMOSTRATIGRAPHIC CORRELATION TOOLS IN THE "MISSISSIPPIAN LIMESTONE" OF THE MIDCONTINENT

By

JUSTIN W. STEINMANN

Bachelor of Science in Earth Science

University of California, Santa Barbara

Santa Barbara, CA

2015

Submitted to the Faculty of the
Graduate College of the
Oklahoma State University
in partial fulfillment of
the requirements for
the Degree of
MASTER OF SCIENCE
July, 2017

ASSESSING THE POTENTIAL OF SULFUR ISOTOPES AND TRACE METALS AS CHEMOSTRATIGRAPHIC CORRELATION TOOLS IN THE "MISSISSIPPIAN LIMESTONE" OF THE MIDCONTINENT

Thesis Approved:

Dr. Natascha Riedinger

Thesis Adviser

Dr. G. Michael Grammer

Dr. James Puckette

Dr. Ben Brunner

ACKNOWLEDGEMENTS

I owe the completion of this project to a great many people who have helped me along the way both with their knowledge and scientific expertise, as well as their encouragement. First and foremost, I want to thank my thesis adviser, Dr. Natascha Riedinger, for her continual support and encouragement for me to strive for more in my work. I am forever grateful that she has given me the opportunity to leave my comfort zone and gain experience in geochemistry. She has taught me how to be a professional geochemist in both my writing and lab work and I am privileged to have worked with her.

I owe many thanks to Dr. Ben Brunner at University of Texas, El Paso, not only for completing my sulfur isotope analysis, but also for lending his expertise in CAS and carbonate geochemistry as well as his sometimes critical, though always valuable, writing critiques.

I would like to thank my committee members, Dr. Michael Grammer, and Dr. James Puckette for their extensive knowledge and expertise. I consider both of them to be legends in their field, and strive to reach a fraction of the level of expertise and experience that they have by the end of my career as a geologist.

I would like to thank the Boone Pickens School of Geology for their financial support, the help that Sandy Earl and the administrative staff has given me, and the ability to learn and work at Oklahoma State University. I also owe thanks to the entire BPSOG geochemistry lab group for their support, especially Doug Ashe, Elliot Hanks, and Devan Grubb for assistance in the field and the lab. I am grateful for having the opportunity to attend OSU and meet and learn from so many great professors and geologists. I also am grateful for the friends that I have made during my stay and hope that I do not lose contact.

I have always been grateful to my parents for their support and encouragement throughout my higher education. Even though they couldn't tell you what I have been researching for the last two years, I know I have always been able to ask them for help if needed. Lastly, I owe more to the love of my life, Alexis, than I could ever repay. She is my number one fan and has sacrificed so much to move here with me, while believing in me every step of the way.

Name: JUSTIN STEINMANN

Date of Degree: JULY, 2017

Title of Study: ASSESSING THE POTENTIAL OF SULFUR ISOTOPES AND TRACE METALS AS CHEMOSTRATIGRAPHIC CORRELATION TOOLS IN THE "MISSISSIPPIAN LIMESTONE" OF THE MIDCONTINENT

Major Field: GEOLOGY

Abstract:

The "Mississippian Limestone" in the Midcontinent, United States, has proven to be a prolific hydrocarbon reservoir and has been intensely studied with regard to lithology, sequence stratigraphy, and facies distribution. Discontinuous lithology and heterogeneous facies of complex carbonate systems, however, make conventional correlation methods, such as lithostratigraphy, difficult. Two novel chemostratigraphic tools may provide a solution to this correlation-challenge: the sulfur isotope composition of carbonate associated sulfate (CAS), which is used as a proxy for the isotope composition of seawater sulfate at the time of carbonate formation and has been successfully applied to reconstruct changes in biogeochemical sulfur cycling on a global scale, and trace metals (TMs), which have been successfully applied in shales as proxies for paleoseawater redox conditions. Utilizing a framework of sequence stratigraphy for the Mississippian limestone in southwest Missouri, we tested the application of CAS isotopes and TM content as correlation tools on samples taken along vertical and horizontal transects from the St. Joe Group. The sulfur concentration and isotope composition of CAS were determined using a leaching and dissolution procedure. The TM content was determined for the carbonate fraction as well as the bulk rock fraction including the siliciclastic phases; samples were analyzed by inductively coupled plasma mass spectrometry. CAS results show a good correlation of the sulfur isotope signal along a lateral transect over hundreds of meters and reflect temporal variations on time scales similar to 3rd-order sequence cycles. The sulfur isotope composition also indicates that the basin was open to global seawater circulation during deposition. Although potential for high-resolution characterization is limited in open ocean basins, CAS isotopes may prove more effective when used for correlation in restricted basin settings. The TM results suggest fluctuating Cd, P, and Ti content on 3rd-order and higher time-scales. The lack of V, U, and Mo enrichments indicate that the rocks were deposited in an oxic environment. Although the effectiveness of CAS and TMs as correlation tools may be limited by the sampling resolution in our study, both parameters can be used to reconstruct the oceanographic conditions of the basin during deposition and thus provide useful information.

TABLE OF CONTENTS

Chapter Page

LIST OF TABLES

Table Page

LIST OF FIGURES

Figure Page

Figure Page

CHAPTER I

INTRODUCTION

The "Mississippian Limestone" in the Mid-Continent has been the focus of a variety of lithological, sequence stratigraphic, and geochemical studies due to its importance as a hydrocarbon reservoir. Extensive carbonate deposition on the Burlington Shelf during the Mississippian resulted in a complex succession of shallow-water and platform-margin to ramp sediments (e.g., Lane and De Keyser, 1980; Gutschick and Sandberg, 1983; Mazzullo and Boardman, 2013; Figure 1). The system has been thoroughly described using traditional techniques including lithology, thin section and outcrop scale facies analysis, and sequence stratigraphy (e.g., Shoeia, 2012; LeBlanc, 2012; Childress and Grammer, 2015) though rapid facies changes and small-scale lithologic heterogeneity can make these methods ineffective when attempting regional correlation. Chemostratigraphy offers another tool with which we may characterize and possibly correlate units. Oxygen and carbon isotopes of carbonates ($\delta^{18}O$ and $\delta^{13}C$) have been used for paleoenvironmental indicators and recently have been tested as regional correlation tools (Koch et al., 2014; Dupont, in press). However, oxygen isotopes can be prone to alteration post-depositional processes such as meteoric diagenesis (e.g, Madhavaraju et al., 2013) and carbon isotopes have been shown to be affected by factors such as changes in carbonate production, diagenetic processes, paleolatitudes, pH, and mineralogy, and may not reflect the depositional isotope composition (Oehlert, et al.,

2012; Wendler, 2013; Dupont, in press). More unconventional geochemical parameters such as sulfur isotope compositions of carbonate-associated sulfate and trace metal abundances have yet to be used in the Mid-Continent, both have the potential to be an effective tool, while avoiding the problems that exist with conventional methods of correlation (Paytan, et al., 2011, and references therein). Sulfur isotopes and trace metals are alternative chemostratigraphic tools that may be used to define chemostratigraphic units and offer a solution to the challenges of regional correlation in heterogeneous systems. Sulfur isotope composition has been used as a paleoseawater proxy to determine ocean basin restriction (e.g., Kampschulte and Strauss, 2004), and may be more resistant to alteration by some diagenetic processes than oxygen or carbon (e.g., Lyons et al., 2004; Gill et al., 2008; Rennie and Turchyn, 2014). Trace metals (TMs) have also previously been used to reconstruct depositional environments and seawater conditions (e.g., Tribovillard et al., 2006) and also may offer a possible tool for correlation when conventional methods such as litho- and sequence stratigraphy are ineffective.

The Burlington Shelf was first described as a thin yet aerially extensive carbonate wedge, several tens to several hundreds of kilometers in width (Lane and Dekeyser, 1980; Gutschick and Sandberg, 1983). More recent work in the Midcontinent has shown it to be more consistent with a carbonate ramp environment (e.g., Mazzullo and Boardman, 2013; Childress and Grammer, 2015), however, for the purposes of this study we will continue to use the "Burlington Shelf" nomenclature when referring to the regional carbonate system. Ramp facies are characterized by thin partially dolomitized crinoidal-bryozoan grain-supported inner ramp facies, undolomitized crinoidal-bryozoan grain-supported mid-ramp facies, and mud-supported argillaceous limestone, wackestone, and cherty mudstone distal

ramp to basinal facies (Lane and DeKeyser, 1980; Childress and Grammer, 2015). Tectonic activity during deposition as well as diagenetic alteration in some areas, overprint the litho, bio-, and sequence stratigraphy of the rocks, complicating an already heterogeneous system (Mazzullo and Boardman, 2013).

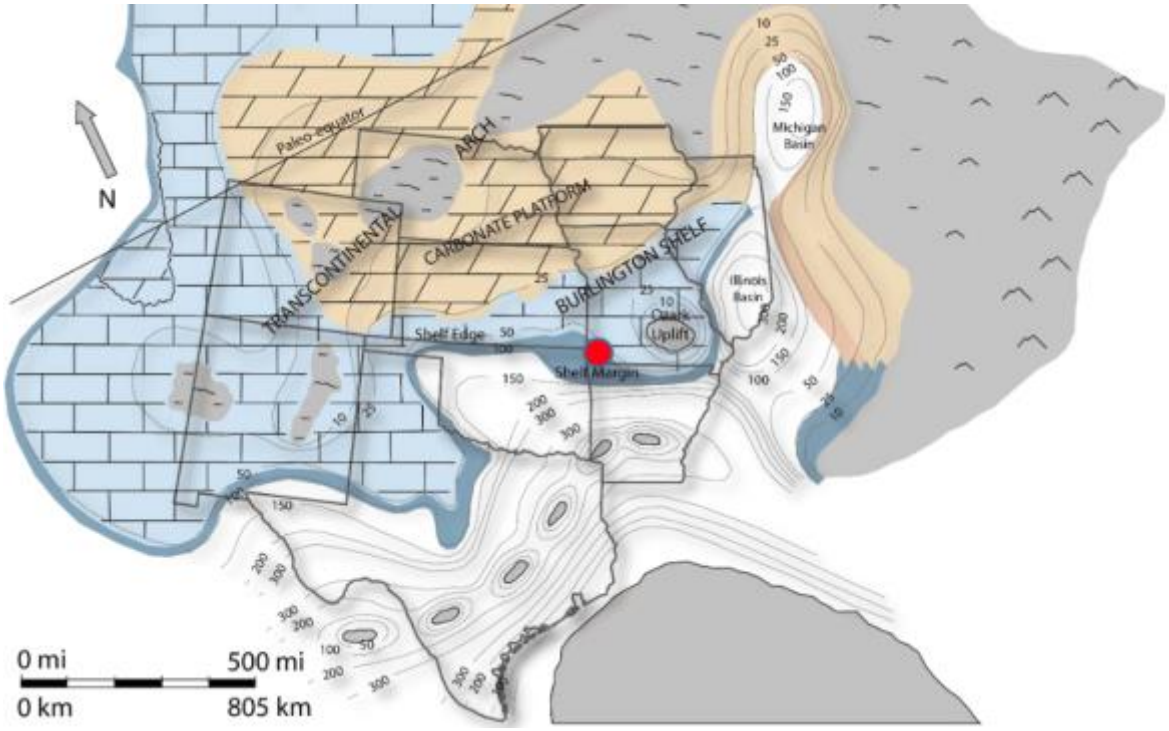

Figure 1: Paleogeographic interpretation of the Mid-Continent during the Early Mississippian. The Burlington Shelf was originally interpreted as a shallow carbonate platform, however more recently has been shown to be consistent with a distally-steepened ramp setting (from Childress and Grammer, 2015). The red dot depicts the location of the study area in southwest Missouri. Bathymetric contours are in meters.

This study uses the "Mississippian Limestone" in the Midcontinent to evaluate the potential of CAS isotope compositions and TM abundances as chemostratigraphic tools that can be used to correlate rock units in heterogeneous systems. We evaluated the temporal and lateral variability of both of these geochemical parameters in order to determine the spatial scale on which they can be used to define strata. This study also provides a geochemical

analysis of the Early Mississippian carbonates using sulfur isotopes and TM abundances to reconstruct the oceanographic and environmental controls on the system during deposition.

Sulfur Isotopes

Sulfur has four stable isotopes (^{32}S, ^{33}S, ^{34}S, and ^{36}S) with ^{32}S and ^{34}S being the most abundant at approximately 95.0% and 4.20 %, respectively (Thode, 1991). Sulfur occurring as sulfate (SO_4^{2-}) is the second most abundant anion in modern seawater, after Cl^- and has a residence time of approximately 10 million years, causing the isotopic composition of sulfur in the global oceans to be effectively homogenous (Rees et al., 1978). However, over geologic time, changes in the concentration and sulfur isotope composition of seawater sulfate have occurred due to changes in the balance of sulfur fluxes. Various geological, geochemical, and biological processes influence the sulfur cycle and subsequently the isotopic composition of the seawater sulfate pool including weathering, continental runoff, volcanism, hydrothermal activity, pyrite burial, and bacterial sulfate reduction (e.g., Thode, 1991; Strauss, 1997; Paytan, et al., 2011; Mills, et al., 2017). One of the most significant fractionation processes for seawater sulfate, bacterial sulfate reduction (BSR), favors ^{32}S, causing residual seawater sulfate to be enriched in ^{34}S. Conversely, the product of BSR, hydrogen sulfide (H_2S), is depleted in ^{34}S and is buried in marine sediment in the form of pyrite and organically bound sulfur (e.g., Thode, 1991). Maximum depletions in ^{34}S of sulfides from populations of sulfate-reducing bacteria were previously thought to be -46‰ (e.g., Rees, 1973; Habicht and Canfield, 2001), though it has since been shown that depletions may reach values above -70‰ (e.g., Wortmann et al., 2001; Brunner and Bernasconi, 2005; Canfield et al., 2010; Sim et al., 2011). Fractionation rates are effected by

temperature variations, substrate type, substrate concentrations, and the bacterial assemblages involved (Canfield, 2001; Sim et al., 2011). The balance between pyrite weathering and pyrite burial has a significant influence on the seawater sulfate isotope composition through time, with pyrite burial being strongly dependent on the intensity of BSR in a system (e.g., Thode, 1991; Strauss, 1997; Paytan, et al., 2011; Tostevin et al., 2014; Mills, et al., 2017).

Previous Sulfur Records

Early data documenting the changing sulfur composition of seawater sulfate ($\delta^{34}S_{seawater}$) through time were obtained from marine evaporite deposits, such as the preliminary time curve presented by Claypool et al. (1980). Evaporites offer limited time resolution/continuity due to their formation in restricted marine settings which may not represent global ocean chemistry, as well as the lack of fossils that can be used for age constraints (Marenco et al., 2008), however, for well-constrained time intervals, evaporites appear to offer a reliable data set (Bernasconi et al., 2017). Marine barite has been used to gather higher resolution sulfur isotope data for the Cenozoic and Cretaceous and additional barite and evaporite data has since been added to the curve, yet significant gaps remained (e.g., Strauss, 1997; Paytan et al., 1998; Paytan et al., 2004). Another method, carbonate associated sulfate (CAS) has been used to analyze sulfur isotopes using the sulfates associated with marine carbonates. Using CAS, sulfur data can be obtained from periods of time and locations where marine barite and evaporites are ineffective or nonexistent.

Carbonate Associated Sulfate

Carbonate associated sulfate refers to the sulfate ions that are bound in a carbonate rock during its formation. Sometimes referred to as 'structurally substituted sulfate' (Kampschulte and Strauss, 2004), it was thought that the sulfate ions (SO_4^{2-}) replace carbonate ions (CO_3^{2-}) in the crystal lattice during mineralization, becoming part of the carbonate structure (Takano, 1985). However, it not certain if this is truly the mechanism for sulfate inclusion, and therefore, the expression 'carbonate associated' may be more appropriate than 'structurally substituted' (Brunner, personal communication, 2015). Sulfate trapped in the carbonate reflects the abundances of ^{34}S versus ^{32}S as well as ^{18}O versus ^{16}O of sulfate ions in the seawater in which the carbonate precipitated (e.g., Burdett et al., 1989; Strauss, 1997; Kampschulte and Strauss, 2004; Marenco et al., 2008, and references therein). No significant isotopic fractionation occurs during CAS incorporation; therefore, analyzing CAS can provide an accurate measurement of the sulfur composition of the seawater during the time of primary carbonate growth (e.g., Burdett et al., 1989; Lyons et al., 2004; Kampschulte and Strauss, 2004; Gill et al., 2007; Gischler et al., 2017). In order to reflect global seawater composition, the basin in which the carbonates formed must have been open to global ocean circulation during carbonate formation. If the carbonates being sampled accumulated within a restricted basin, or seaway closed off from global circulation, the CAS will represent the composition local to that basin (e.g., Burdett et al., 1989; Kampschulte and Strauss, 2004). For the analysis of global seawater sulfate, CAS from well-constrained biogenic carbonates formed within a basin open to global circulation offers a more precise sulfur isotope analysis than that of marine evaporites, and is more widespread than marine barite (Paytan et al., 2011).

Carbonate associated sulfate offers an improved spatial and temporal distribution of data as well as better precision than previous marine sulfate data, yet limitations still exist. The accuracy with which CAS represents the seawater sulfate composition is dependent on the condition of the carbonates it is extracted from, and therefore the effect of post-depositional alteration, including diagenesis and dolomitization, must be considered (e.g., Marenco et al., 2008; Gill et al., 2008; Paytan et al., 2011). Marenco et al. (2008) found that trends exist between the degree of dolomitization and sulfur isotope compositions, where limestones exhibit higher $\delta^{34}S_{CAS}$ values than dolomitized rocks. During dolomitization, original calcite may be replaced with dolomite with a sulfur isotope composition that does not correspond to sulfate from seawater during original deposition, and instead reflects that of the dolomitizing fluid during alteration. CAS may remain valid for dolomitic rocks, though the degree of dolomitization and alteration history must be considered. Early marine diagenesis does not seem to affect the CAS sulfur isotopic signals in the same way, and the signal remains representative of formation conditions despite influence from pore waters and bacterial sulfate reduction (Lyons et al., 2004; Gill et al., 2008; Rennie and Turchyn, 2014). Gill et al. (2008) showed that meteoric diagenesis lowers the concentration of CAS. However, during sulfate removal, no stable sulfur isotope fractionation occurs and thus, the remaining CAS preserves the original sulfur isotope signature and therefore is not compromised by meteoric diagenesis (Gill et al., 2008). Since the sulfate molecule is very stable, and does not exchange oxygen isotopes with water (e.g., Rennie and Turchyn, 2014), it is reasonable to presume that also the oxygen isotope composition of CAS remains undisturbed. Any sulfate introduced during authigenic carbonate precipitation are sourced from the original rock, and therefore the original sulfur isotopic signal is preserved, though concentrations may decrease (Gill et

al., 2008). However, if calcite crystallization occurred from sulfate-laden non-marine diagenetic fluids, the resulting sulfur and oxygen isotopes may not reflect that of the originally deposited rock. This must be considered when working on rocks with a history of fluid flow or diagenetic overprint. Though more work is needed to understand the effects of diagenesis on CAS, early marine or meteoric diagenesis has been shown to not significantly compromise the CAS sulfur isotopic signal.

Trace Metals

Similar to sulfate, trace amounts of elemental metals may also be incorporated into the carbonate structure and reflect metal concentrations of the seawater during the time of precipitation (Hastings et al., 1996; Beer et al., 2011). Although present in seawater in very low concentrations, usually below 1 ppm (Bruland and Lohan, 2003), the abundances and states of these trace metals (TMs) can be used to determine a variety of paleoenvironmental conditions (e.g., Reeves and Brooks, 1978; Tribovillard et al., 2006, and references therein). Most commonly, elements such as vanadium (V), molybdenum (Mo), and uranium (U) have been used to evaluate redox conditions in paleomarine systems (Hastings et al., 1996; Tribovillard et al., 2006; Algeo and Rowe, 2012). Redox condition refers to the state of oxidizing agents (oxygen) in the system, and in turn, the biogeochemical processes that control the distribution of oxygen. Redox conditions can be described as being oxic ($[O_2]>2$ ml/l H_2O), suboxic ($2>[O_2]>0.2$ ml/l H_2O), and anoxic ($[O_2]=0$ ml/l H_2O). Euxinic is used to describe conditions where $[O_2]=0$ ml/l H_2O but with measurable amounts of free H_2S present (e.g., Tyson and Pearson, 1991; Tribovillard et al., 2006). Under anoxic and euxinic conditions, V, U, and Mo become enriched in the sediment (Figure 2; Algeo, and Maynard,

2004). Therefore, TM content measured for V, U, and Mo can be used to determine the paleoredox conditions of the basin during deposition.

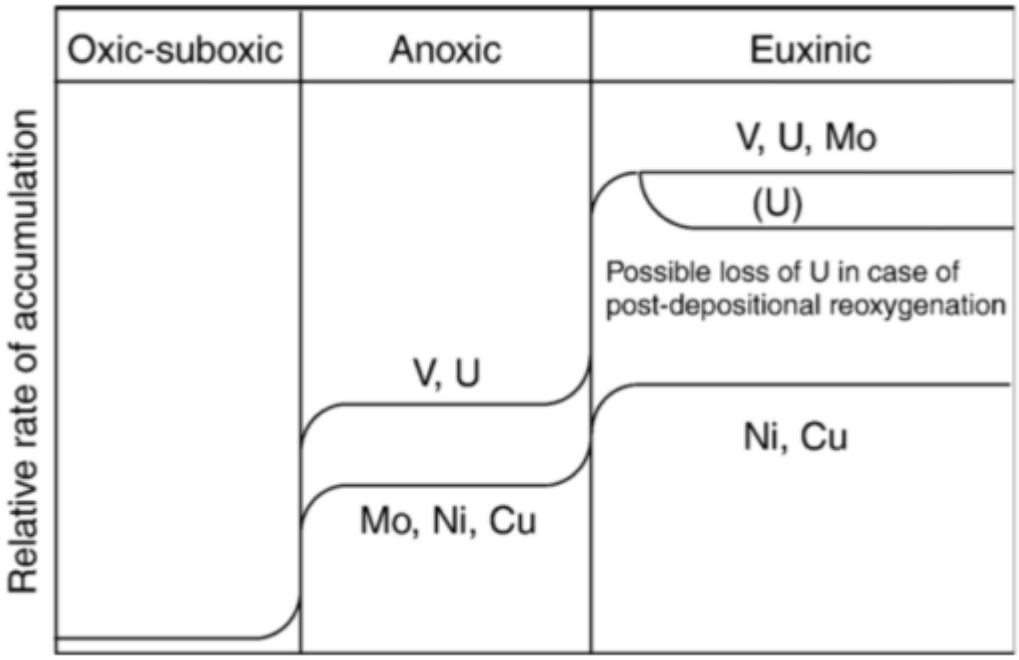

Figure 2: Diagram showing relative enrichments of certain TMs when transitioning from oxic-suboxic to anoxic and euxinic conditions (From Tribovillard et al., 2006).

Other metals such as chromium (Cr), and cobalt (Co) are influenced by detrital input and therefore may indicate sources of detrital input (Tribovillard et al., 2006). Nickel (Ni), copper (Cu), zinc (Zn), and cadmium (Cd) are used as micronutrients in biogeochemical cycles or are associated with organic matter, making them useful as paleo-productivity proxies (Tribovillard et al., 2006, and references therein). Each specific trace metal plays a different role in the ocean's biogeochemical cycle, therefore a suite of trace metal data may give crucial insight into the paleoseawater conditions in which the sample was deposited.

TM abundances have already been developed into a tool for recognizing changing hydrographic conditions or anoxic/oxic events within a basin (e.g., Algeo and Rowe, 2012,

and references therein). Trace metal enrichments or depletions caused by such an event can be recognized in samples throughout the basin, and therefore chemostratigraphic boundaries can be defined. Few studies, such as Guo, et al. (2007) have applied the same concept to widespread TM enrichments in shales, to correlate areally extensive units within a basin. Further developing this tool, TMs signatures within a stratigraphic section may be used as an additional parameter to characterize and correlate rock units. Much the same way lithofacies are defined, geochemical facies may be defined using trace metal assemblages. Finding trends in TM abundances, or similar geochemical facies, a rock unit may be correlated between locations within a basin, even when lithology varies. TMs show potential to be used as a chemostratigraphic tool in which to characterize and correlate rocks, and may be used in conjunction with other tools such as sulfur isotope compositions to provide an effective characterization.

What Makes an Effective Stratigraphic Correlation Tool?

In order to assess the potential of a new chemostratigraphic tool, we must first define what makes an effective chemostratigraphic tool. Chemostratigraphy refers to the classification and correlation of sediment and rock packages based on their geochemical compositions (Ramkumar, 2015). Both isotope stratigraphy and TM stratigraphy aim to define rock units based on their geochemical characteristics; the first using isotope compositions, and the second using TM abundances. The approach is similar to that of lithostratigraphy, where rocks are grouped and distinguished based on lithology. For lithostratigraphy to be effective, rock units must be characterized based on a trait (grain size, composition, sorting, etc.) that can be distinguished from the surrounding strata, as well as if it is laterally continuous so that

it can be correlated between locations. The temporal scale at which these units must be distinguished and the lateral scale on which they must be continuous depends on the question addressed. The same is true for chemostratigraphy, where the geochemical parameter – or suite/set of geochemical parameters – being used must be distinguishable from the surrounding strata, though consistent enough laterally that it may be correlated with strata at other locations. An ideal chemostratigraphic correlation tool will use a parameter (set) that varies frequently and distinctly between strata, and is laterally consistent within a single unit. The higher the frequency with which this parameter varies, the higher the frequency cycles or higher resolution time-scales that will be able to be defined using it. Similarly, the scale in which the parameter is laterally continuous will determine the spatial scale on which it can be used to correlate (outcrop, region, basin, global). Also, if a parameter is affected by syn- or post-depositional processes in a way that makes it inconsistent within a rock unit, it has limited use as a correlation tool.

CHAPTER II

METHODS

Study Area

The study location was chosen due to the existence of a detailed sequence stratigraphic framework from a previous study (Childress and Grammer, 2015). The study area consists of two outcrops located on the north side of Highway 71 near Jane, in McDonald County, Missouri. The southern sampling location, nearest to Jane, is the outcrop studied by Childress and Grammer (2015) to develop their sequence stratigraphic framework for the Mississippian strata in Missouri, and will be referred to as the "Primary" outcrop. The Primary outcrop lies 0.5 km northwest of the intersection of Highway 71 and Route 90, 20 km east of the Oklahoma – Missouri border (36° 32' 49'' N, 94° 19' 32'' W; Figure 3). The outcrop consists of a road cut, which exposes a section of Woodford Shale and Lower Mississippian strata 250 m long, and 20 m high, oriented northwest-southeast, at an elevation of 306 m above sea level. The outcrop is bordered on the northwest by a private road, and on the southeast by a soil-covered slope. The second sampling location, referred to as the "Secondary" outcrop, lies 0.5 km northwest of the Primary outcrop along Highway 71 (36° 33' 5'' N, 94° 19' 53'' W), consisting of a several hundred-meter-long road cut exposing Mississippian strata stratigraphically above that of the Primary outcrop.

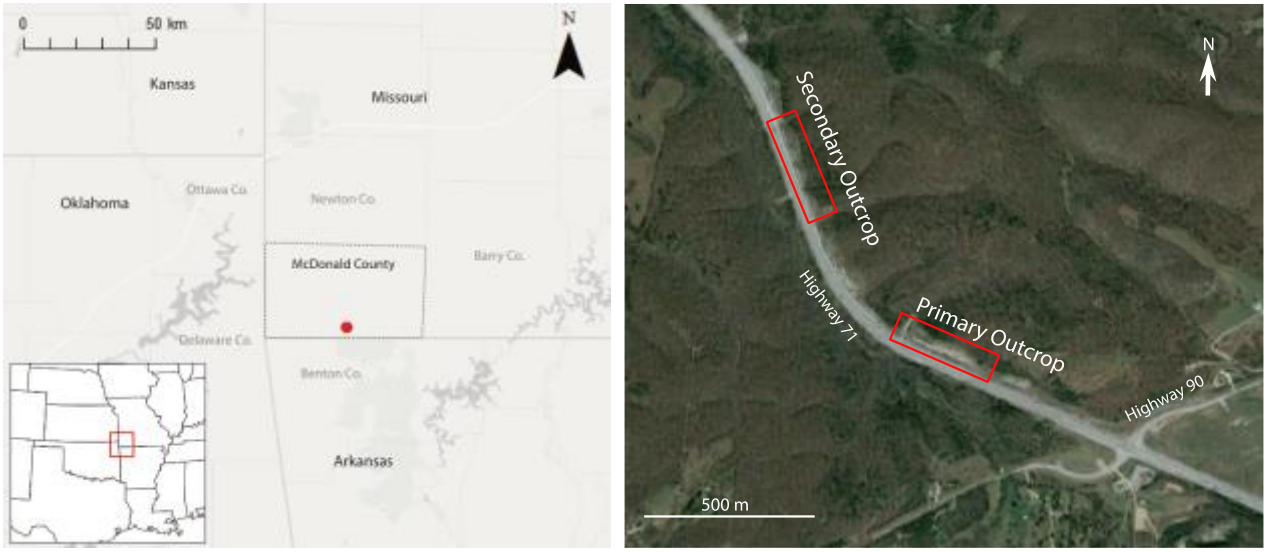

Figure 3: Left, overview of the Midcontinent, United States. The study area is shown by the red dot. Right, location of Primary and Secondary outcrops along Highway 71, in southwest Missouri.

Stratigraphic Framework

The lithology at the study area is consistent with a distally-steepened ramp setting, with deep-water deposits to the southwest (Mazzullo and Boardman, 2013). The dominant facies include calcareous shale to silty limestone, and crinoidal-bryozoan wackestones, packstones, and grainstones, deposited on the middle ramp (See Figure 1). The studied stratigraphy consists of the upper Devonian section of the Woodford Shale, and the overlying Mississippian strata including the Bachelor, Compton, Northview, and Pierson formations. Samples were collected from the Compton, Northview, and Pierson formations, which make up the Kinderhookian-Osagean St. Joe Group (Figure 4; Mazzullo and Boardman, 2013; Childress and Grammer, 2015).

At the Primary outcrop, the Bachelor Fm. unconformably overlies the Woodford Shale (Figure 4; Childress and Grammer, 2015). The Bachelor Fm. appears as a thin green-gray bed of calcareous shale reaching no more than 10 cm in thickness, nonexistent in some locations. The Compton Fm. overlies the Bachelor Fm. and appears in the outcrop as a 3-4 m

thick, thickly bedded section of crinoidal-bryozoan wackestones, packstones, and grainstones. The Compton Fm. contains several allochthonous masses that have most recently been interpreted as olistoliths carried downslope by debris flows and deposited in a mid-to-lower carbonate ramp setting (Childress and Grammer, 2015). These olistoliths were avoided during sampling as they may not represent the geochemical characteristics of the surrounding deposits. The Northview Fm. is the uppermost Kinderhookian strata and is seen as a 0.5 to 2 m thick bed of green-gray calcareous shale to silty limestone. Childress and Grammer (2015) notes that flaser bedding, lenticular bedding, bi-directional ripples, and exposure surfaces are present within the Northview Fm. at the study location, indicating a

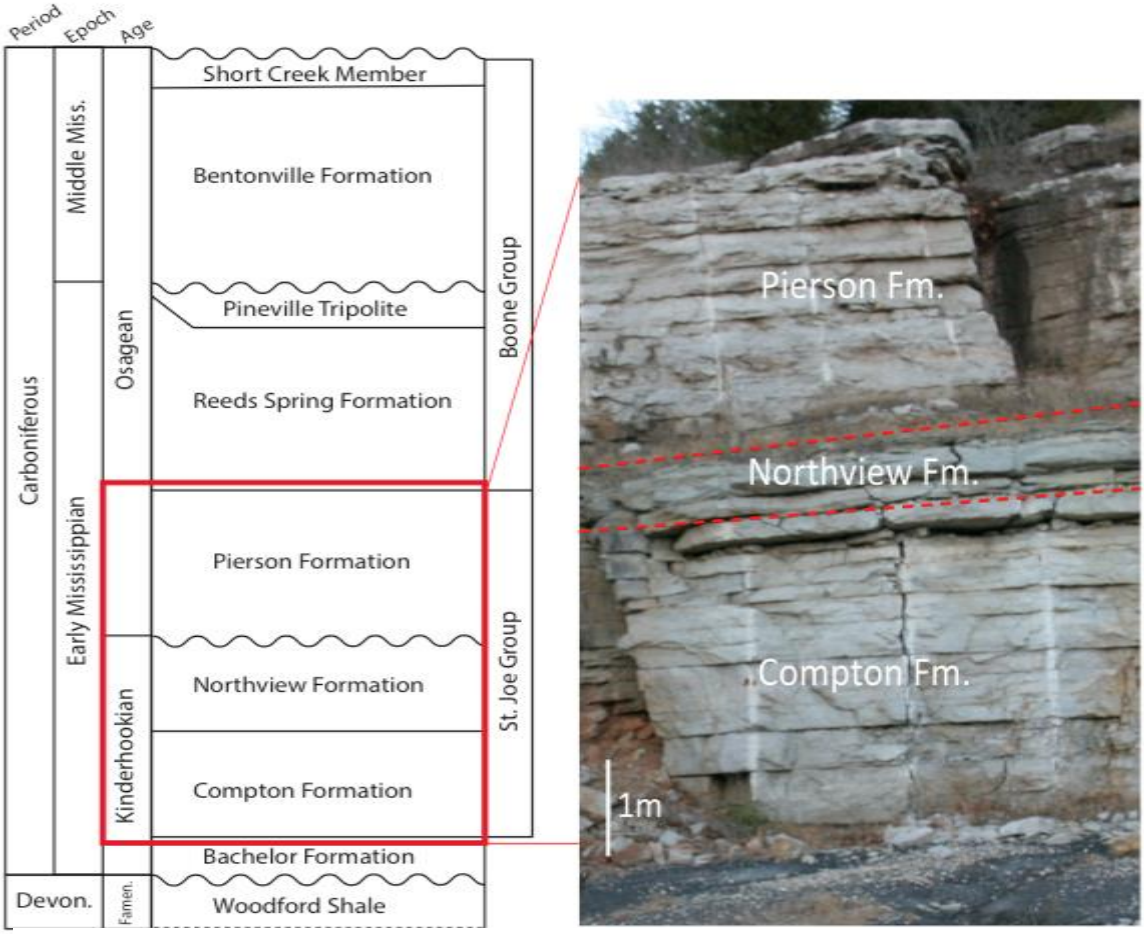

Figure 4: Stratigraphic column and outcrop picture showing the sampled strata. Samples were taken from the Compton, Northview, and Pierson formations of the St. Joe Group. Stratigraphic column based on Mazzullo and Boardman (2013).

shallowing upward tidal flat depositional environment. The Osagean Pierson Fm., Osagean in age, is the uppermost unit of the St. Joe Group and unconformably overlies the Northview Fm. It consists of 4-6 m of crinoidal-bryozoan packstones and crinoidal grainstones. The lithology is similar to that of the Compton, yet the Pierson Fm. displays an increased variability of skeletal grains, including brachiopods, bryozoans, and ostracods, and lacks olistoliths such as those observed in the Compton (Childress and Grammer, 2015). Overlying strata at the top of the outcrop are covered by soil and vegetation.

Thin section analysis completed for the outcrop (Childress and Grammer, 2015) indicates skeletal grain abundance ranging from 30% to 85%, with the highest percentages in what were interpreted to be the most proximal, shallow-water facies. Micrite matrix composed approximately 5% in the most proximal facies, and up to 65% in the mud-rich distal facies. Cement ranges from 2-10% and usually consist of blocky calcite crystals. Dolomite rhombs are present in some facies but typically less than 5% and localized. Pyrite and dead oil are present, but usually less than 1% filling fractures and vugs. Fracture, vuggy, interparticle, and intraparticle pore types were present; sizes were on the nano- to micro-pore scales and overall porosity is usually less than 1% (Childress and Grammer, 2015).

The Secondary outcrop consists of Pierson strata that in hand sample appear to be a finer-grained wackestone-packstone, lighter in color, and contains fewer fossils than that at the Primary outcrop. The Pierson Fm. is overlain by the Osagean Reeds Spring Fm., which consists of fine-grained and sparsely fossiliferous gray limestone (Cline, 1934) with up to 75% blue-gray syndepositional and post depositional chert, and is the lowermost unit of the Boone Group (Mazzullo and Boardman, 2013). In this region, the contact between the Reeds Spring and underlying Pierson Fm. is an angular unconformity (Mazzullo and Boardman,

2013) although in other regions the Reed Springs overlies the St. Joe Group conformably (Cline, 1934).

Although significant complexity and heterogeneity exist within the system, the facies present within the St. Joe Group strata are most consistent with those deposited on a distally-steepened ramp, between fair-weather and storm wave base (Figure 5; Childress and Grammer, 2015, and references therein).

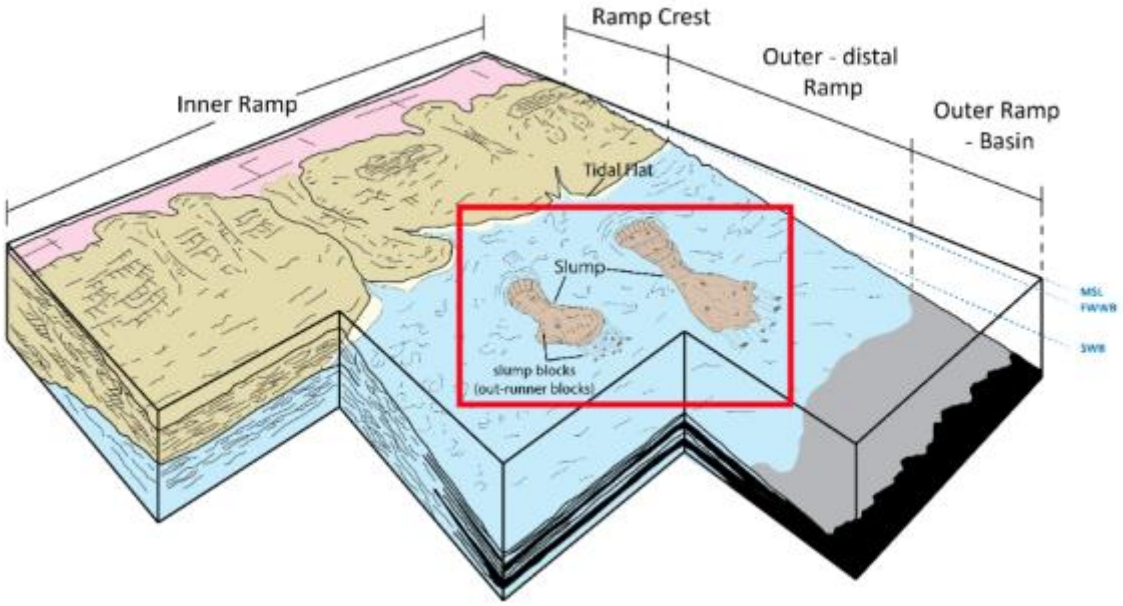

Figure 5: Depositional model for the study area as proposed by Childress and Grammer (2015) and shown by a red box. Facies are consistent with being deposited on a distally-steepened ramp between fair-weather (FWWB) and storm wave base (SWB). The most proximal facies include those of the tidal flat deposits within the Northview Fm. The large masses within the Compton Fm., interpreted as slumps, were deposited on the outer-distal ramp setting (From Childress and Grammer, 2015, modified from Handford, 1986).

For the purpose of this study, cycle hierarchy will be defined as presented by Kerans and Tinker (1997) (Table 1). Transgressive phases are defined by deep-water crinoidal-bryozoan wackestone facies, while regressive phases are defined by shoaling upward facies including crinoidal-bryozoan wackestones, packstone-grainstones, and skeletal grainstones (Childress and Grammer, 2015). Two 3rd-order sequences were defined and remained consistent across the outcrop. The first 3rd-order sequence includes a transgressive phase spanning the entire

thickness of the Compton Fm., and a regressive phase spanning the thickness of the Northview Fm. The Northview Fm. is capped by a subaerial exposure surface, representing the greatest extent of sea level fall observed in this outcrop. The transgressive phase of the second 3rd-order sequence begins at the base of the Pierson Fm., indicated by an exposure horizon and implied flooding surface just above the Northview Fm. The regressive phase begins just over 1 m above the Pierson-Northview boundary, and continues for the rest of the outcrop. Multiple 4th- and 5th-order high frequency cycles are superimposed on the 3rd- order sequences, though are less continuous across the outcrop (Childress and Grammer, 2015).

Table 1: Table showing the cycle hierarchy for sea level sequences and cycles (From Childress, 2015; after Kerans and Tinker, 1997).

Cycle Hierarchy				
Tectono-Eustatic Cycle Order	**Sequence Stratigraphic Unit**	**Duration (n = my)**	**Relative Sea Level Amplitude (m)**	**Relative Sea Level Rise/Fall Rate (cm/1000 yrs)**
First	Supersequence	> 100		< 1
Second	Supersequence	10 – 100	50 – 100	1 – 3
Third	Depositional Sequence, Composite Sequence	1 – 10	50 – 100	1 – 10
Fourth	High-Frequency Sequence, Parasequence, and Cycle Set	0.1 – 0.4	1 – 150	40 – 500
Fifth	Parasequence, High-Frequency Cycle	0.02 – 0.04	1 – 150	60 – 700

Field Methods

Samples were taken from the Primary outcrop at 0.3 – 1 m intervals along vertical transects previously studied by Grammer and Childress (2015). Samples from the secondary

outcrop were taken along a lateral northwest-trending transect in an attempt to assess lateral variability. Samples were taken from the upper Pierson Fm. using the contact defined in Shoeia (2012), and by the lack of chert characteristic to the Reeds Spring Fm. (Appendix, Figure 13). Sample locations at this outcrop were approximately 25 m apart, and less than 1 m below a distinct silty marker bed to ensure that samples were taken from the same stratigraphic horizon (Figure 6). When possible, samples were taken with a Pomeroy EZ Core hand-held gasoline powered core drill with diamond-tipped core bit. This allowed us to take samples from deeper within the outcrop, in an attempt to avoid weathering rinds and exposed surfaces. With this method, short cores 1 inch in diameter and 2-6 inches long, with minimal weathering rinds were recovered. In the following discussion, 'cores' will refer to these short cores taken using the hand held drill. In locations where cores were not obtainable, hand samples were taken using a rock hammer. Hand samples were large enough to ensure that there was sufficient material for processing after weathered surfaces were removed from the sample. In some locations, cores as well as hand samples were taken to evaluate the effect of each collection method.

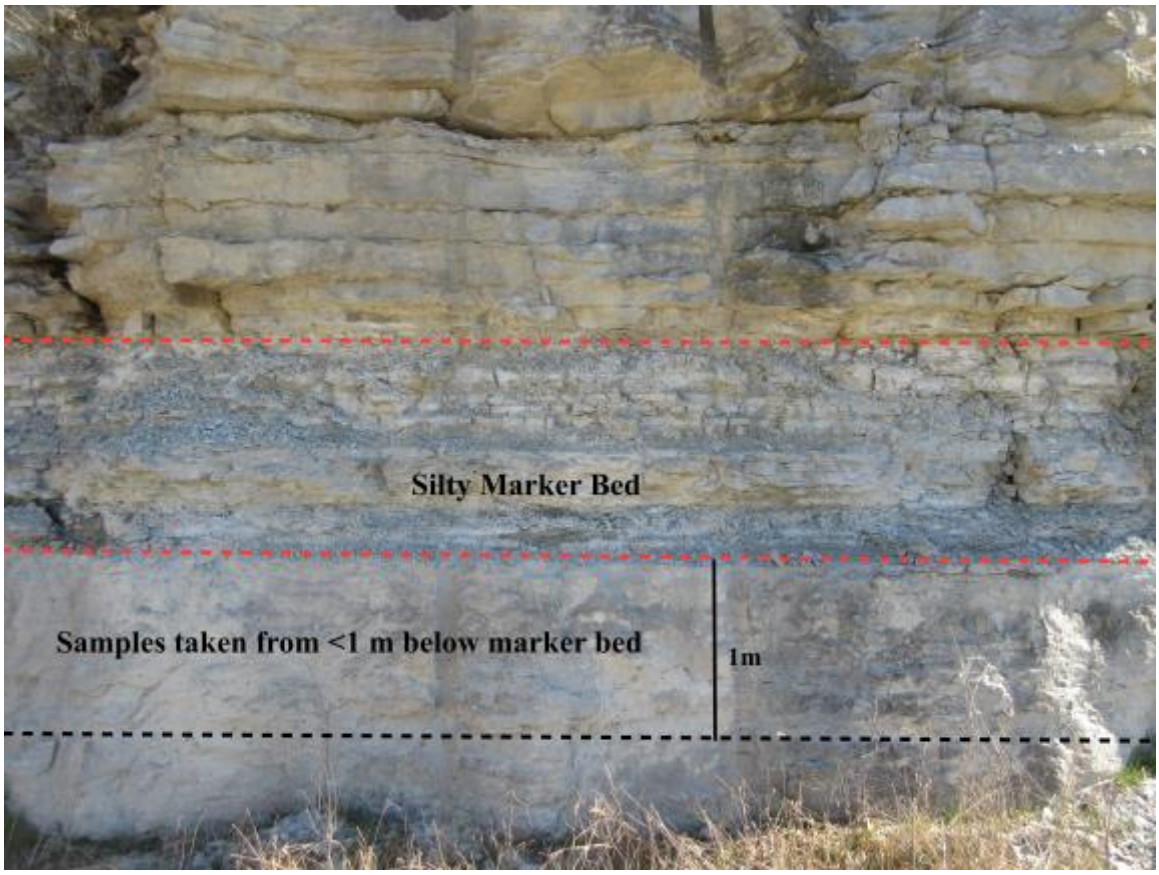

Figure 6: Photo of the Secondary outcrop. Samples for the lateral transect were taken within the Pierson Fm., no more than 1 m from the silty marker bed, though typically within 10-30 cm.

CAS Analysis

Short cores and hand samples taken from the field were analyzed for CAS sulfur isotope compositions. A rock saw was used to cut away all visible weathered edges and secondary veins. Samples were first broken using a rock hammer, and then crushed into a fine homogeneous powder using a ball mill with a steel canister.

Samples used for CAS analysis were prepared using methods modified from those presented by Kampschulte and Strauss (2004) and Gellatly and Lyons (2005). Wotte et al., (2012) and Theiling and Coleman (2015) presented further methods to ensure proper rinsing

and prevent oxidation of the samples during dissolution, yet the method described below was found to be sufficient in this study. Whole rock and core samples were washed and cut into slices with a rock saw to remove any veins and weathered edges. The rock slices were crushed using a ball mill until finely powdered. Between 20-40g of the powdered sample (dependent on the amount available) was added to an Erlenmeyer flask, along with 500 ml of 10% NaCl solution. The solution was thoroughly shaken by hand, and then left to soak for 12 hours. The purpose of soaking in NaCl solution was to remove any soluble sulfate minerals such as gypsum from the sample (Kampschulte and Strauss, 2004). The samples were then decanted and soaked in 500 ml deionized water for 24 hours to rinse away the NaCl solution. Next, 500 ml of 5.25% NaOCl was added and left to soak for 48 hours followed by decanting and two 24 hour DI water rinses. The NaOCl leaching removes any organically bound sulfur present in the samples (Gellatly and Lyons, 2005). The samples were completely dissolved with 4M HCl and filtered with a 0.45 micron Millipore vacuum filtering system. The residue remaining after HCl dissolution was weighed and recorded as insoluble. Next, 125 ml of saturated (250 g /L) barium chloride solution was added to each flask and left to precipitate until visible barium sulfate settled to the bottom of the flask (2-3 days). The solutions were then vacuum filtered, where the barium sulfate was recovered using a pre-weighed Millipore filter. After drying overnight in an oven at 40° C, barium sulfate was recovered from the filters and transferred to vials. When possible, all samples from a single transect were prepared during the same set to minimize procedural variability. A modern sample, either ooids from the Bahamas, or shells from San Diego, CA, was prepared with each set to use as a modern reference. After extraction, approximately 0.5 mg of barium sulfate from each sample was weighed into a 5mm x 9mm tin combustion capsule along with 0.5 mg of

vanadium pentoxide, sealed, and placed in a well plate. All CAS sample preparation and extraction was completed at Oklahoma State University using facilities and lab supplies provided by Boone Pickens School of Geology.

Prepared samples were sent to the University of Texas at El Paso's Department of Geological Sciences to be analyzed for sulfur isotope composition using an Elementar GeoVisIon® continuous flow isotope ratio mass spectrometer (CF-IRMS) attached to an Elementar Pyrocube® elemental analyzer. Sulfur isotope data is expressed as a δ-value (‰) relative to the sulfur isotope ratio for the Vienna Canyon Diablo Troilite (VCDT) standard, as defined:

$$\delta^{34}S = \left\{ \frac{(^{34}S/^{32}S)_{sample} - (^{34}S/^{32}S)_{standard}}{(^{34}S/^{32}S)_{standard}} \text{ X } 1000 \text{ ‰} \right\}$$

To determine the error in the CAS extraction and measurement method, repeats for several of the samples were measured, including a triplicate of three samples from the Primary outcrop, a triplicate of one sample from the Secondary outcrop, and a duplicate of one sample from the modern samples. Error was calculated by using the standard deviation of the mean for all repeat samples. The maximum error for $\delta^{34}S_{CAS}$ was determined to be ± 0.21‰ for the Primary outcrop. The error for the Secondary outcrop was ± 0.06‰, and for the modern samples was ± 0.15‰. It is important to note that repeat samples were split after barium sulfate precipitation, therefore additional error between samples introduced during the earlier stages of leaching and extraction may not be fully represented by this error calculation.

Analytical error introduced from the instrument was determined separately using lab standards. Maximum instrument error was determined to be ± 0.18‰.

Trace Metal Analysis

In order to determine the TM abundances associated with different phases in the samples, a two-step TM analysis was carried out. Separate extractions were completed on trace metals associated with the carbonate fraction, and the bulk fraction, including siliciclastic and other non-carbonate minerals. Short cores collected from the field were drilled using a Dremel rotary tool and a 1/8 inch diamond-coated carbide drill bit, producing a fine powder, which was placed in a sealed vial. Material was taken from the interior of the sample using the drill so as to minimize inclusion of contamination of the sample during coring.

For sample digestion, 250 mg (± 1 mg) of each sample was added to a cleaned teflon vial. For the carbonate-only fraction, a leaching procedure modified from methods presented by Tessier et al. (1979) and Poulton and Canfield (2005) was used. Samples were leached in a 1 M sodium acetate solution that was acidified to a pH of 4.0 using acetic acid and shaken for 24 hours. For bulk fraction TM content, a multi-acid total digest procedure with nitric (HNO_3), hydrochloric (HCl), and hydrofluoric (HF) acid using a temperature and pressure digest system (PicoTrace, DAS) was used. The abundances of trace metals in each fraction were measured via inductively coupled plasma-mass spectrometry using a Thermo Fisher Scientific ICAP Qc MS®. All trace metal sample preparation and analysis was completed at Oklahoma State University. TM-grade equipment, containers, and chemicals were used during the digestion and analysis of the samples to avoid introducing metal contamination during the procedure. Trace metal abundances are reported in ppm and the analytical error

for each fraction is calculated using the standard deviation of a set of repeat measurements. Average analytical error for the bulk-fraction samples is ± 2.0 %; average error for carbonate-fraction is ± 1.3 %.

For bulk-fraction TM abundances enrichment factors (EF) were calculated by normalizing the TM content to the aluminum content, and comparing to an average shale:

$$EF_{TM}=(TM_{sample}/Al_{sample})/(TM_{shale}/Al_{shale}).$$

Average shale values were taken from Wedepohl (1971). Though the samples rocks are not shale, Wedepohl's (1971) values for average shale were used for normalization because little data exists on the average trace metal composition of carbonates.

CHAPTER III

RESULTS

CAS Data

Sulfate Concentrations

Sulfate concentrations [SO_4^{2-}] were calculated gravimetrically from the mass of barium sulfate precipitated, and the original mass of the sample used. This calculation gave a sulfate concentration of the sample, assuming that the sample was 100% carbonate minerals. Many samples contained various amounts of clay and silica minerals that were not dissolved during HCl dissolution, and were not reflected in the calculated sulfate concentration. Samples ranged from greater than 99% carbonate minerals for the modern samples, to as low as 40% for the siltier Northview Fm. samples. Carbonate percentage was calculated using the recovered mass of insoluble residue and the total sample mass. During the initial CAS extraction runs, the insoluble residue was not recorded for some of the samples. The percentage of carbonate for these samples was estimated using the percentage calculated for the known sample from the closest stratigraphic interval to the unknown sample. Error may exist in cases where there is small-scale variation in lithology. The calculated sulfate concentrations were corrected for all samples in this way.

The $[SO_4^{2-}]_{CAS}$ for the Primary outcrop range from 87 ppm to 976 ppm with an average of 344 ppm and a standard deviation of 177 ppm (Figure 7). For the Secondary outcrop, samples taken over a single lateral transect yielded $[SO_4^{2-}]_{CAS}$ from 233 ppm to 975 ppm with an average of 459 ppm and a standard deviation of 176 ppm (Figure 8).

Sulfur Isotope Compositions

Sulfur isotope values were obtained from 59 samples of the Mississippian limestone in the study area (Appendix, Table 2). Of these, 39 were taken from the Primary outcrop along vertical transects, and 20 from the Secondary outcrop along a lateral transect. For the Primary outcrop, $\delta^{34}S_{CAS}$ values range from 7.4‰ to 25.8‰, with an average of 20.8‰ and a standard deviation of 3.9‰ (Figure 7). Values increase from approximately 18‰ in the Compton Fm. (Early Kinderhookian) to 23‰ in the Northview Fm. (Late Kinderhookian), and decrease again in the middle Pierson Fm. (7-10 m) to approximately 16‰. For the lateral transect, $\delta^{34}S_{CAS}$ values range from 12.1‰ to 21.6‰ with an average of 15.8‰ and a standard deviation of 2.7‰ (Figure 7). The two locations with the heaviest $\delta^{34}S_{CAS}$ values are 65 m (19.9‰) and 83 m (21.6‰). For both of these locations, additional samples taken from the same location fall closer to the average $\delta^{34}S_{CAS}$ for the lateral transect ($\delta^{34}S_{CAS}$ 13‰ and 16‰).

Modern Samples

A sample of modern carbonate sediment was prepared and analyzed with each lab set as a control. Modern samples were either ooids from Joulter's Cay, Bahamas, or carbonate shell debris collected near San Diego, California, composed of over 99.8% carbonate. The $\delta^{34}S$

values for the modern samples were from 20.9 – 22.3‰ with an average value of 20.8‰. All of the modern carbonates yielded values that lie reasonably close to the accepted value of 20.6‰ (Rees, 1978), and a recently determined value for the eastern Pacific Ocean basin of 21.24‰ (Tostevin, et al., 2014). There were no significant differences in the $\delta^{34}S_{CAS}$ values of the two sample locations, as would be expected considering the sulfur isotope composition of the global ocean is assumed to be homogeneous. The modern control samples were treated the same way through the lab procedure as the study samples, and the resulting values show that the lab procedure is successful in measuring accurate $\delta^{34}S_{CAS}$ values.

Concentration data was also calculated for the modern samples, which varied between the Bahamian and the Californian samples. The average value for the Bahamian samples is 2830 ppm while the Californian average is 1760 ppm. The accepted modern global seawater sulfate concentration is approximately 2780 ppm (Millero, 2005; Algeo et al., 2015), however, seawater sulfate concentrations are dependent on local processes such as continental freshwater input and sediment source, and therefore may vary globally, especially near shorelines (Thode, 1991). Additionally, sulfate incorporation is dependent on the carbonate component being formed (Staudt and Schoonen, 1995). For example, Staudt and Schoonen (1995) show that mollusks tend to incorporate less sulfate as CAS than ooids, which may explain the difference in concentration between the Bahamian ooids and the Californian shells. Although varying between location, concentrations for multiple samples from the same location were consistent (within approximately 250 ppm), supporting the methods reproducibility.

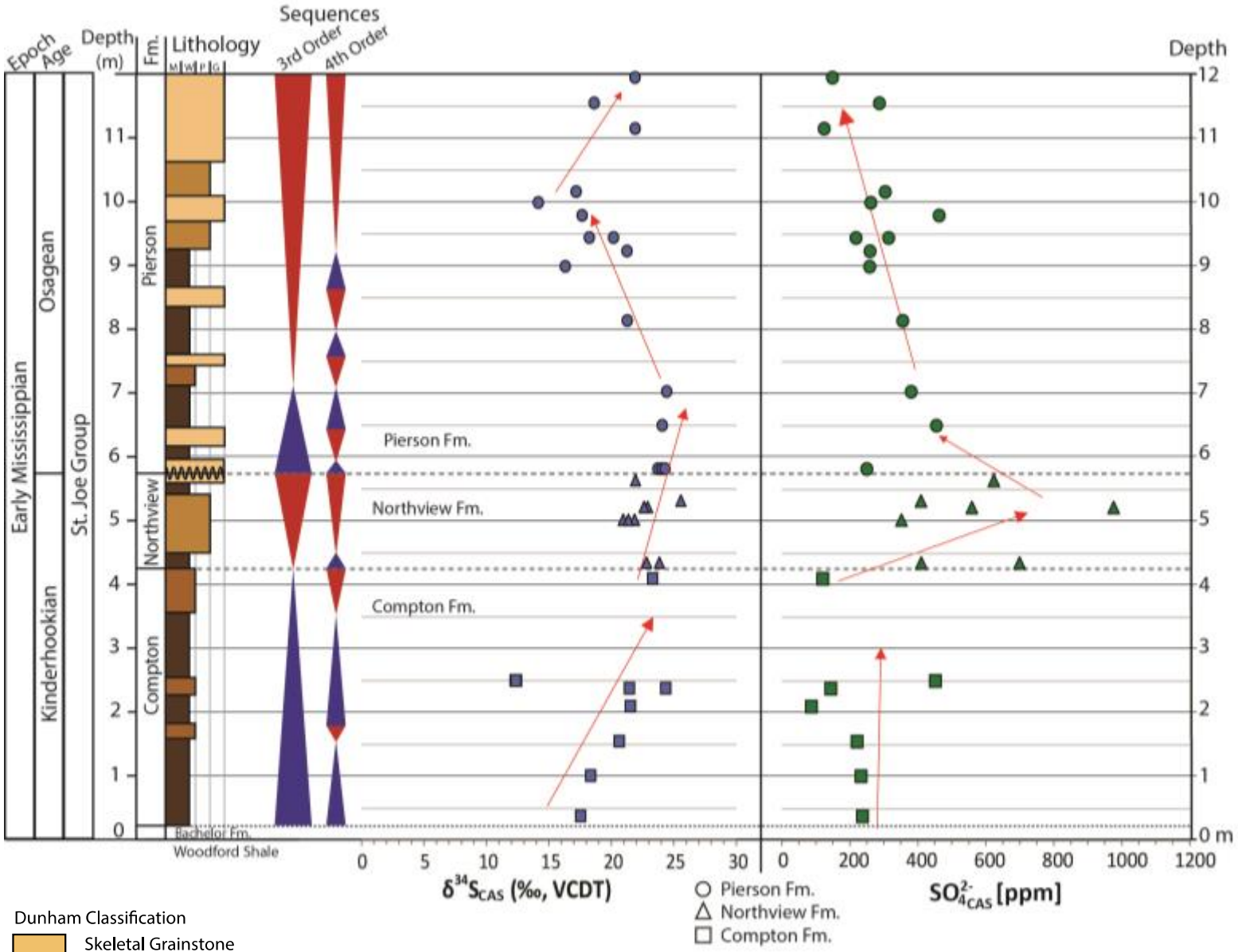

Figure 7: $\delta\ ^{34}S_{CAS}$ and $[SO_4^{2-}]_{CAS}$ for Vertical Transect 2**.** Lithology and sequence cycles taken from Childress and Grammer (2015). Arrows show trends up the section. Lithology based on the Dunham (1962) classification for carbonates.

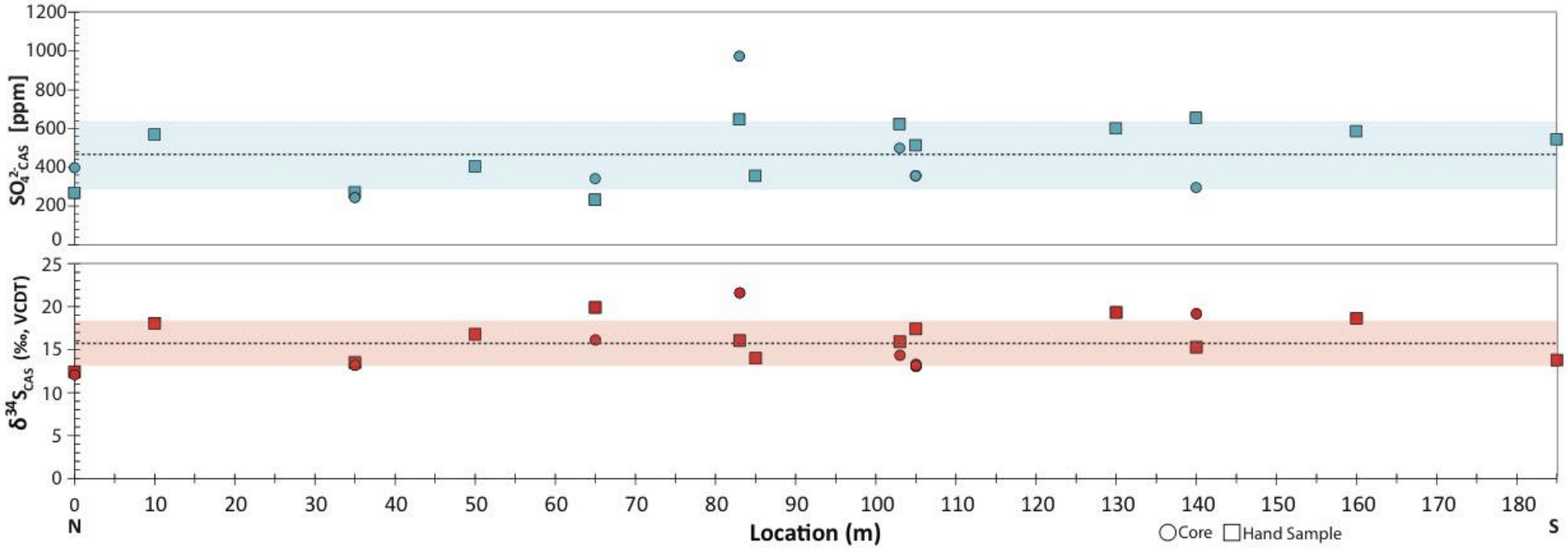

Figure 8: $\delta^{34}S_{CAS}$ and $[SO_4^{2-}]_{CAS}$ for the lateral transect plotted against sampling location from north (0 m) to south (185 m). Dashed lines represent mean of each dataset; shaded bars represent standard deviation from the mean of each dataset. All samples were taken from the Pierson Fm. stratigraphically above that of the vertical transect

Trace Metal Data

Vertical Transect TM Content

Bulk-fraction and carbonate-only fraction TM abundances were obtained from samples along vertical transects of the primary outcrop for 15 elements. All values reported here are taken from a single vertical section (VS2; Figure 9). Phosphorous (P) bulk-fraction abundance for all samples in VS2 varies between 48.75 and 228.73 ppm while carbonate-fraction abundance varies between 18.18 and 59.31 ppm. The P carbonate-fraction abundance shows a decreasing trend from 0 m to 2.5 m approximately 80 to 60 ppm), and a similar increase from 4 m to 6 m. Titanium (Ti) bulk-fraction abundance varies between 706.30 and 882.80 ppm while carbonate-fraction abundance varies between 171.67 and 321.61 ppm. Carbonate-fraction Ti abundance fluctuates between the minimum and maximum values on 2-3 meter-scale cycles. Bulk-fraction trends follow decreasing carbonate-fraction Ti abundance from 5.75 m to 7 m, and increasing trends from 10 m to 12 m. Vanadium (V) bulk-fraction varies between 1.40 and 9.07 ppm and carbonate fraction varies between 0.21 and 7.58 ppm. Chromium (Cr) bulk-fraction contents vary between 0.97 ppm and 4.35 ppm and the carbonate-fraction varies between 0.13 and 4.74 ppm. Nickel (Ni) bulk-fraction varies between 2.73 and 35.55 ppm while the carbonate-fraction varies between 0.76 and 32.84 ppm. Uranium (U) bulk-fraction content varies between 0.03 and 0.09 ppm and carbonate-fraction content varies between 0.01 and 0.04. Vanadium, Cr, Ni, and U, have different absolute contents, though they share similar trends. The carbonate-fraction of these elements show decreases of similar magnitude over the interval from 0 to 2 m. Vanadium and Cr carbonate-fractions both spike in abundance at approximately 5 m (200-300%), but then

return to the previous values. The abundances remain relatively consistent for the rest of the section. The bulk-fraction abundance for V and Cr steadily increase from 5.75 m to 7 m, during the same interval where bulk-fraction Ti abundance decreases (Figure 8). Vanadium and Cr peaks at 10 m follows this increasing trend, though due to the low sample density, we cannot say whether this is truly a trend or a single anomalous sample. Thorium (Th) bulk-fraction varies between 0.17 and 0.73 ppm and the carbonate-fraction varies between 0.06 and 0.98 ppm. The molybdenum (Mo) bulk-fraction content is low (< 0.27 ppm) while the carbonate-fraction is consistently below the detection limit of the instrument. Cadmium (Cd) bulk-fraction varies between 0.14 and 0.37 ppm while the carbonate-fraction varies between 0.09 and 0.41. Carbonate-fraction Cd abundance increases from approximately 0.1 ppm (100 ppb) to over 0.3 ppm from 4 m to 7 m and then decreases again to approximately 0.2 ppm from 7 to 10 m. Barium (Ba) bulk-fraction varies between 3.26 ppm and 49.52 ppm and, except for an outlier (49.52 ppm), remains relatively consistent through the section (0-10 ppm). Carbonate-fraction Ba abundance varies between 1.15 and 22.41 ppm. Additional metal abundances can be seen in the Appendix (Table 4 and 5).

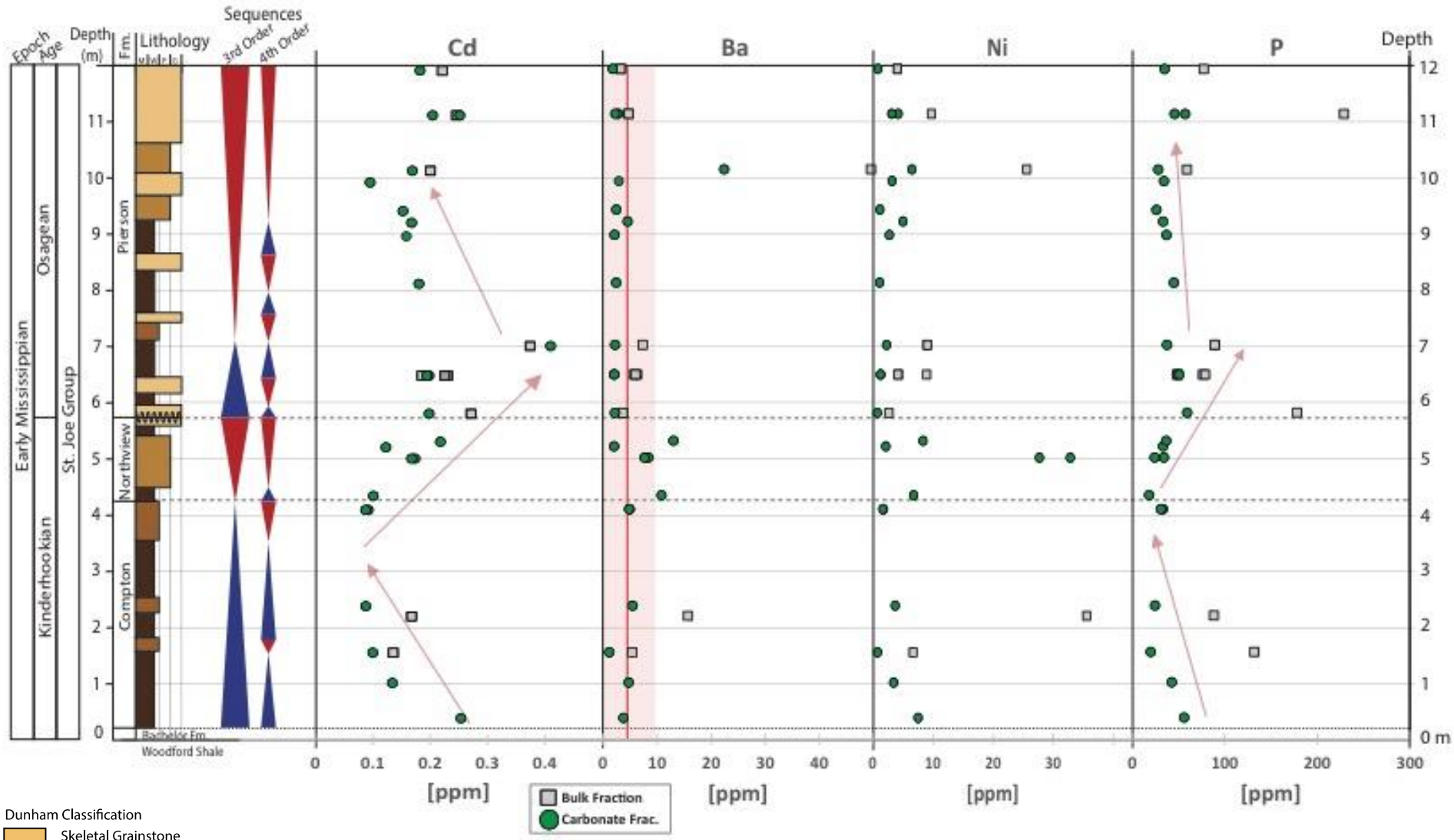

Figure 9: Trace metal content for both bulk- and carbonate-only fractions plotted against stratigraphic height, facies, and sequences (Childress and Grammer, 2015). Arrows for Cd, P, and Ti, show generalized trends in abundance. For Ba, the red line indicates mean while the shaded area represents one standard deviation from the mean to signify relative lack of deviation. Continued on next page.

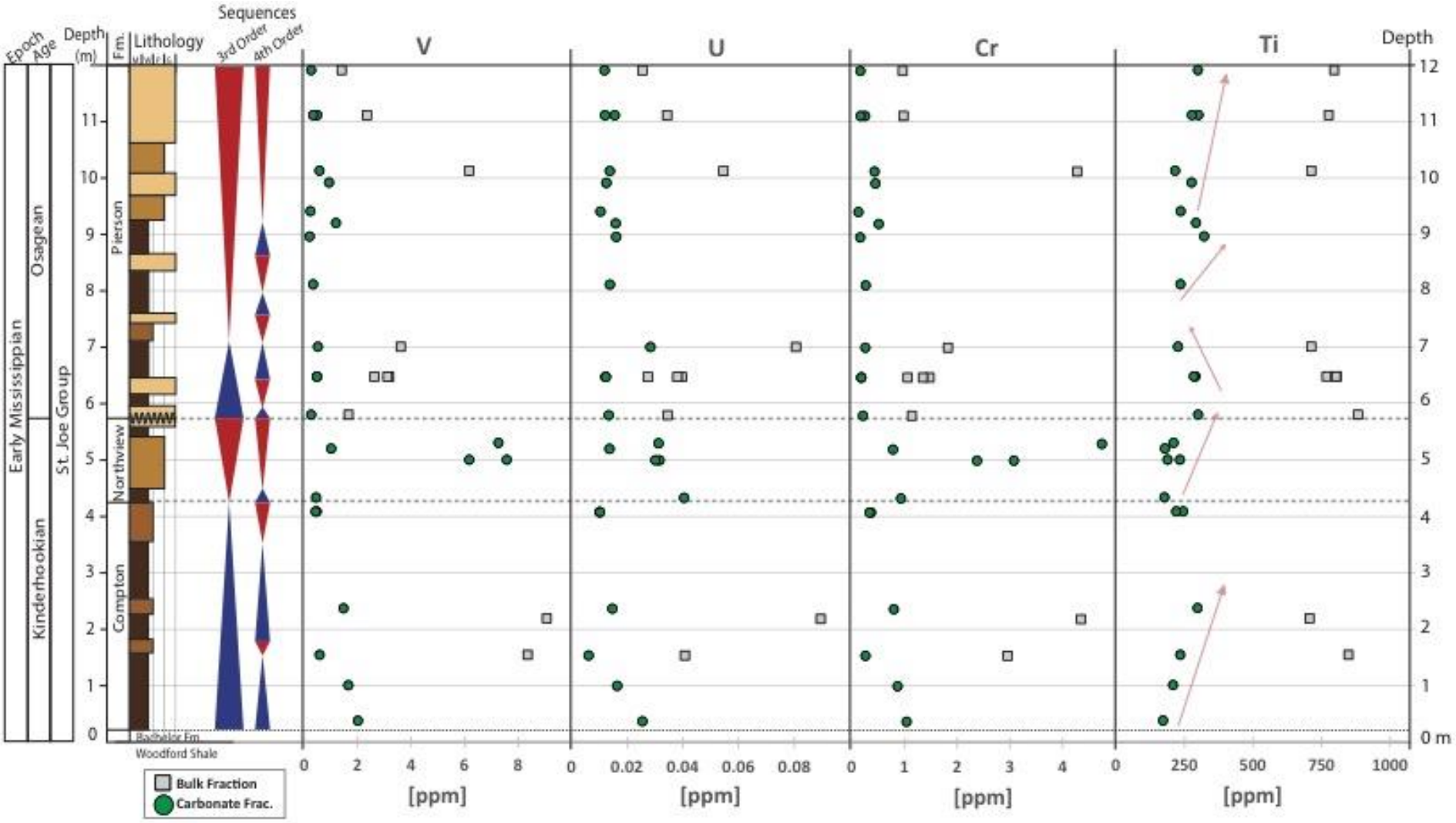

Dunham Classification

- Skeletal Grainstone
- Crinoidal-Bryozoan Packstone
- Crinoidal Wackestone-Packstone
- Crinoidal-Bryozoan Wackestone

Figure 9, continued: Trace metal content for both bulk- and carbonate-only fractions plotted against stratigraphic height, facies, and sequences (Childress and Grammer, 2015). Arrows for Cd, P, and Ti, show generalized trends in abundance. For Ba, the red line indicates mean while the shaded area represents one standard deviation from the mean to signify relative lack of deviation.

Enrichment Factors

The enrichment factor (EF) for each element was calculated and is provided in the Appendix, (Table 6). Samples from two transects (VS2 and VS3) were included for EF data. Enrichment factors greater than 1 indicate enrichment relative to average shale; conversely, EFs less than 1 indicate depletion (e.g., Tribovillard et al., 2006). Phosphorous and Cd both show an enrichment over the section; P with EF's between 1.87 and 26.85 and Cd between 27.05 and 278.72. Cadmium shows the highest enrichment out of any measured TM. Vanadium, Cr, Fe, Mo, and Th all show negligible enrichments with EFs ranging from 0.76 to 4.41, with average EFs between 1.0 and 2.0. Barium shows an average EF of 0.76, with individual samples ranging from 0.39 to 2.18. Uranium is also generally depleted with an average EF of 0.70, with samples ranging from 0.33 to 2.19. No apparent trend is seen moving up the section for the EF of any mentioned TM.

CHAPTER IV

DISCUSSION

CAS Sulfur Isotope Composition

Temporal Variability

The sampled vertical transects contain approximately 15 Ma of strata – from the Early Kinderhookian through the Mid-Osagean (Childress and Grammer, 2015; Boardman et al., 2013. Both $\delta^{34}S_{CAS}$ and $[SO_4^{2-}]_{CAS}$ values obtained from VS2 appear to occur over similar stratigraphic intervals as the 3rd-order sequences presented by Childress and Grammer (2015) (Figure 7). Increasing $\delta^{34}S_{CAS}$ from the base of the Compton Fm. to the Northview Fm. occur during the same interval as the established 3rd-order transgressive phase (Figure 7), while decreasing $\delta^{34}S_{CAS}$ values occur at the onset of the 3rd-order regressive phase within the Pierson Fm. A slight decrease in $\delta^{34}S_{CAS}$ values could also correlate with the 3rd-order regressive phase within the Northview Fm. No patterns are visible between the $\delta^{34}S_{CAS}$ values and higher-frequency cycles, suggesting that the $\delta^{34}S_{CAS}$ may not vary on high-frequencies. The $[SO_4^{2-}]_{CAS}$ values remain relatively constant during the 3rd-order transgressive phase of the Compton Fm. defined by Childress and Grammer (2015), though increase abruptly during the regressive phase within the Northview Fm. Values consistently decrease again during the regressive phase of the Pierson Fm. (Figure 7) With the limited

data, it is unclear if these trends are influenced by changes in sea level and therefore show consistent relationships between sulfur composition and regressive/transgressive phases. A drop in sea level and subsequent regression could cause partial restriction in a basin. Restriction of a basin, and subsequent evaporation, may result in increasing salinity, and therefore higher sulfate concentrations. Basin restriction could be a probable cause of the increase in $[SO_4^{2-}]_{CAS}$, though the same trend during the regression in the Pierson Fm. cannot be observed. The Northview Fm. is described as a proximal tidal flat environment (Childress and Grammer, 2015), and contains a significantly higher amount of silt and clay than the surrounding strata. It is therefore a more probable explanation that the increase in $[SO_4^{2-}]_{CAS}$ is caused by a higher continental input, which would could cause a local increase of dissolved sulfate in the seawater.

Lateral Variability

The $\delta^{34}S_{CAS}$ values across the lateral transect show good correlation over the 185 m lateral transect. Most samples lie within one standard deviation from the mean, and they show consistent deviation from the mean across the outcrop (Figure 8). The data show that there is no recognizable trend when moving laterally from one location to another on the 100 m scale. At 0 m from north, and 35 m from north, hand samples and cores taken from the same location show $\delta^{34}S_{CAS}$ values within 0.4 ‰, showing that there is little difference in isotope composition between hand samples and cores. However, at other locations such as 65 m, hand samples and cores show differences in $\delta^{34}S_{CAS}$ values up to 5.6‰. The difference in values is likely due to sub-meter scale localized variations in the isotope composition of the rocks, as the samples were taken close, though not exactly in the same location. Sulfate

concentrations show variation (233-974 ppm), though there is no recognizable trend moving from one side to the other. Similar to the $\delta^{34}S_{CAS}$ values, the deviation from the mean is consistent for $[SO_4^{2-}]_{CAS}$ across the outcrop, with the exception of an outlier at 83 m which lies at nearly 1000 ppm. (Figure 8). These consistent $[SO_4^{2-}]_{CAS}$ values indicate that both depositional and diagenetic processes affecting sulfate concentration acted uniformly for the sediments across the outcrop, and that additionally to the $\delta^{34}S_{CAS}$ $[SO_4^{2-}]_{CAS}$ may be used for outcrop-scale unit characterization.

Paleogeographic Implications

Aside from evaluating its chemostratigraphic potential, the results of this study can be used to reconstruct paleoenvironmental and paleogeographic conditions, during the Mississippian. By comparing the $\delta^{34}S_{CAS}$ values obtained in this study to sulfur isotope compositions compiled in the global seawater record (e.g., Strauss, 1997; Kampschulte and Strauss, 2004; Paytan, 2011), we can evaluate the connectivity of the basin in which the studied strata were deposited to the global oceans. Previously compiled global sulfur isotope values obtained from evaporites, marine barite, and whole rock CAS for Early Mississippian seawater range from 20‰ to 24‰ (Figure 10; e.g., Strauss, 1997; Kampschulte and Strauss, 2004; Paytan, 2011). The average value for $\delta^{34}S_{CAS}$ from the vertical transect (20.39‰), which is Early Mississippian in age, lies within this range. The global record also shows a decrease in $\delta^{34}S$ from the Kinderhookian (approximately 355 Ma ago) to 15‰-17‰ in the Late-Osagean (approximately 340 Ma ago). The average $\delta^{34}S_{CAS}$ obtained from the Secondary outcrop is 15.8‰, therefore the data in this study is consistent with the decreasing

trend of $\delta^{34}S$ through the Early Mississippian (Figure 9). This decrease in $\delta^{34}S$ values may be the result of a decline in BSR during the transition from greenhouse to icehouse conditions (Haq and Schutter, 2008; Childress and Grammer, 2015). The sulfur isotope compositions obtained for the study outcrops match those expected for the global ocean seawater sulfate, implying that the studied strata were deposited in a basin open to global ocean circulation

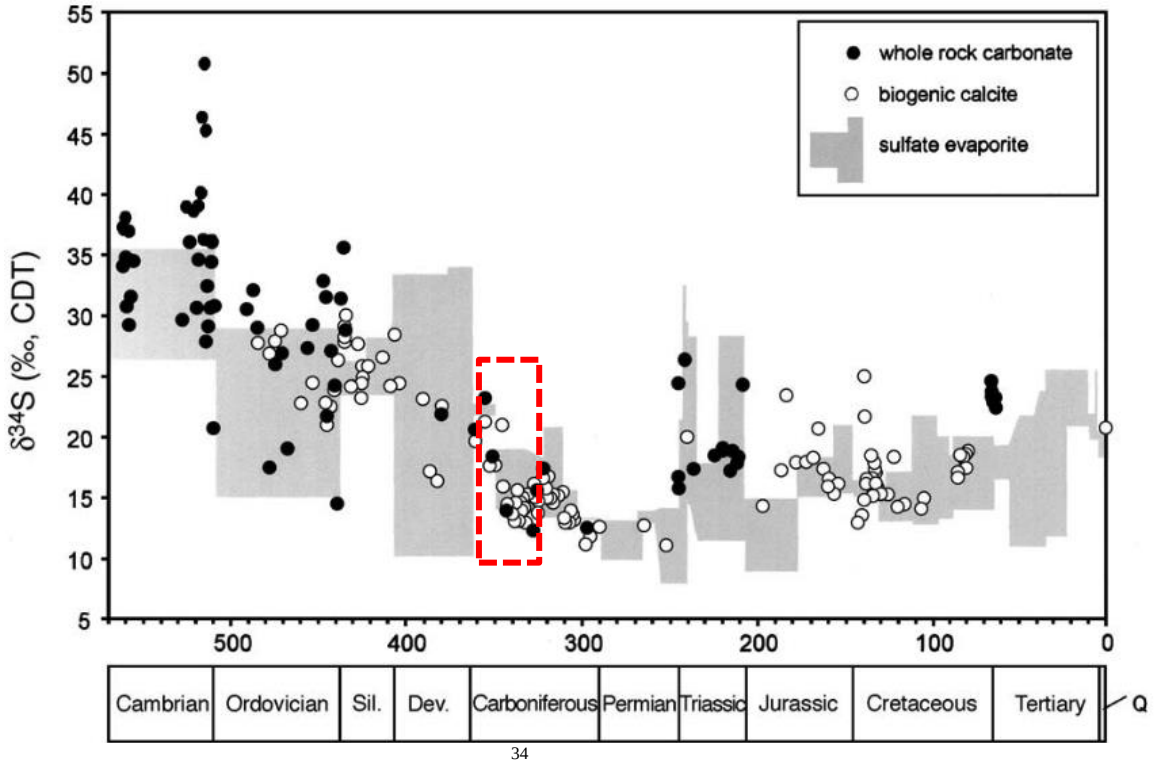

Figure 10: Compilation of global seawater $\delta^{34}S$ values. Values from the study lie within the range of previously published values for the Early Mississippian, shown by the red box. Samples from this study decrease from 20.4 ‰ in the Early Kinderhookian to 15.8 ‰ in the Osagean, matching the global seawater trend (Modified from Kampschulte and Strauss, 2004).

during the Early Mississippian. Previously discussed paleogeographic interpretation for the Mississippian shows the carbonate ramp flanked to the south by an open ocean basin, and subject to global seawater circulation (Gutschick and Sandberg, 1983; Childress and Grammer, 2015). The $\delta^{34}S_{CAS}$ findings in this study support this paleogeographic interpretation.

Though the $\delta^{34}S_{CAS}$ values for this study generally match those of the global sulfur record, there may have still been periods of partial restriction. Localized restriction due to high frequency (<5 Ma) sea level fall may have occurred at some point and may be responsible for some of the variations in $\delta^{34}S_{CAS}$ values within the vertical section that deviate from the overall global seawater trend. Work completed on the Mississippian limestone at other locations in the Midcontinent may also deviate from the global trend due to these localized sub-basin restrictions in seawater circulation. However, the overall trend shows that the carbonate ramp at this location was predominantly open to global ocean circulation during the Early Mississippian.

Chemostratigraphic Potential of CAS

The sulfur compositions for the Early Mississippian carbonates within the study area fluctuate on frequencies that appear to be similar to that of previously established 3rd-order sequences (Figure 7). Occurring over such low-frequency cycles, no distinct enrichment or depletions in $\delta^{34}S_{CAS}$ are seen that may be used for high-frequency correlation. The long residence time of sulfate in the global ocean (10 Ma) along with the large volume of the global ocean sulfate pool does not allow for high-frequency (<5 Ma) or high magnitude fluctuations in the sulfur composition of seawater. Therefore, these data show that $\delta^{34}S_{CAS}$ would not be effective at correlating units on high-frequency time-scales for the Mississippian carbonates. However, $\delta^{34}S_{CAS}$ may be used for global correlation in conjunction with the global sulfur record on 3rd-order and lower-frequency time scales (>5 Ma).

The chemostratigraphic implications discussed above apply to the Mississippian carbonates deposited on the mid-ramp environment of the Burlington Shelf, which, based on the recent paleogeographic interpretation (Childress and Grammer, 2015), as well as the $\delta^{34}S_{CAS}$ data from this study, was implied to have been open to global ocean circulation. Sulfur isotope compositions are of limited use for correlation when studying sediments deposited in open ocean basins, however, they may be more effective in correlation on higher-frequency cycles when obtained from sediments deposited in restricted basins (Bergersen, 2016). A restricted basin, one that is cut off either partially or entirely from the global oceans would receive limited, or no sulfate input from the global sulfate pool. Without receiving sufficient replenishment from global oceans, bacterial sulfate reduction occurring in a restricted basin could cause the seawater sulfate sulfur composition to be enriched in the basin relative to global oceans (e.g., Chen et al., 2013; Sælen et al., 1993). The sulfate pool of the restricted basin would be a smaller volume, and more susceptible to frequent perturbations in the sulfur cycle, resulting in higher-frequency variations (e.g., Gill et al., 2007; Chen et al., 2013). These high-frequency cycles may be seen as shorter-duration (<5 Ma), higher magnitude, enrichments and depletions in the sulfur isotope composition, and therefore may be used to characterize and correlate higher temporal resolution rock units than this study indicates. Bergersen (2016) suggests a similar idea, noting that correlation success would be dependent on developing a high resolution seawater record for the basin, in conjunction with using a high sampling density. Therefore, the potential remains for sulfur to be used as an effective correlation tool when working in rocks that were deposited within a single restricted basin.

Impact of Diagenetic History

In order for $\delta^{34}S_{CAS}$ values obtained from our samples to be used in chemostratigraphic correlation or paleogeographic reconstruction we must be confident that these values reflect the chemistry of seawater during deposition, and not post-depositional fluids or diagenetic events that may have occurred. Therefore, it is important to understand the diagenetic history of any rocks in which sulfur isotopes are analyzed. The Mississippian rocks in the Midcontinent have been proposed to have a complex diagenetic history (Morris et al, 2013; Mohammadi et al., 2017), which could have possibly altered the sulfur isotope composition. Thin section analysis by Childress and Grammer (2015) found blocky calcite cement (<10%) suggesting the possibility of dissolution and remineralization during meteoric or burial diagenesis (Flügel, 2010). If the calcite cement was a result of meteoric fluids moving through the system, the sulfate concentration may have been lowered, though the isotope composition would be preserved, as no new sulfate was introduced into the system (Gill et al., 2008). Dolomite rhombs are present, though they rarely make up more than 2% of sample mineralogy and are usually localized; therefore, dolomitization was not extensive (Childress and Grammer, 2015).

Studies completed on Early Mississippian rocks in Missouri and Oklahoma using oxygen and carbon isotopes indicate multiple diagenetic and cementation events (Morris, et al., 2013; Mohammadi et al., 2017). Morris et al. (2013) recognized several different cement types with distinct oxygen and carbon isotope compositions, though attributed all to early marine or meteoric cementation. As mentioned before, early marine cementation would represent that of the depositional seawater, and episodes of meteoric dissolution and precipitation may affect sulfate concentrations, though would not affect sulfur isotope composition. However,

in addition to early marine and meteoric cements, Mohammadi et al. (2017) found oxygen and carbon compositions of calcite and dolomite cements to be consistent with late diagenetic events sourced from basinal fluids. The authors propose that saline fluids from underlying Ordovician rocks migrated upward into Mississippian strata during episodes of late-diagenesis.

Stable oxygen and carbon isotope composition of carbonate samples collected from the studied outcrop (Sessions, 2016) points to minimal impact of diagenesis. Sessions (2016) concluded that isotopic overprinting had not occurred for oxygen or carbon and that the obtained values represent the depositional isotopic composition of the rocks. An evaluation of the oxygen and carbon values obtained for the Primary outcrop revealed that compositions match those determined to be meteoric and early marine by Mohammadi et al. (2017; Appendix, Figure 18).

Therefore, although Mohammadi et al. (2017) and Morris et al. (2013), suggest a complex diagenetic history for the Mississippian rocks in the Midcontinent, the rock formations sampled for this study do not appear to have undergone any significant diagenesis that would have altered the sulfur isotope composition (Childress and Grammer, 2015; Sessions, 2016; Mohammadi et al., 2017). Further in support of the study area having undergone limited diagenetic alteration, is that the $\delta^{34}S$ match those of the global ocean for the Early Mississippian, as well as reflecting the global depletion of $\delta^{34}S$ values into the mid-Osagean.

Trace Metal Content

Cadmium, P, and Ti show apparent trends in TM abundance that may be used to reconstruct paleoenvironmental changes through time, and be tied to sequences or distinct rock units. Cadmium shows the most distinct trends in both bulk-fraction and carbonate-fraction TM content that appears to correspond with the established 3rd-order sequences (Childress and Grammer, 2015), though peak enrichments and depletions are offset from sequence boundaries (Figure 8). Higher-frequency variations may exist, though the sampling interval limits the resolution in which these trends can be recognized. Phosphorous appears to follow similar 3rd-order frequency cycles, matching those of Cd. Given that the outcrop covers approximately 15 Ma of time, these cycles occur on 5-10 Ma time-scales suggesting that changes in productivity occurred on similar time scales and are reflected in the Cd and P content of the rocks.

Titanium possibly shows temporal trends on higher-frequencies than Cd and P. Figure 8 shows Ti abundance fluctuating on 1-3 m intervals – similar time scales as the established 4th-order frequencies. Though some 1-m cycles seen in the Ti record appear to match the frequency of the 4th-order high-frequency sequences presented by Childress and Grammer (2015), limited data makes it unclear whether they correlate with the exact sequence boundaries. It is even less clear whether these variations in Ti abundance are influenced by these sequence cycles, or rather the effect of a different process such as sediment input or biogeochemical processes. From this data there is no apparent relationship with regressive or transgressive phases, however, it does appear that 4th-order cycles of longer duration (seen from 0-3 m and 9-12 m) correspond with Ti abundance trends of longer duration. Other TMs abundances may also change through time and have relationships with sequences or

lithology, though the obtained data is not high enough resolution to draw any stratigraphic relevant conclusion.

Some trace metals (Al, Ti, Cr, Co) are strongly tied to the detrital input, whereas others (Ba, Cd, P) are more affected by productivity processes occurring within the water column (e.g., Tribovillard et al., 2006, and references therein). Those that are highly influenced by detrital input may be affected by sea level changes as the amount of continent-derived sediment input changes from lowstand to highstand. Determining which fractions a TM is primarily associated with can aid in determining its origin, and whether or not it is strongly tied to detrital input. The element's relationship with Al is useful in determining detrital influence as Al is thought to be of primarily detrital origin, and usually immobile after deposition (Calvert and Pederson, 1993; Hild and Brumsack, 1998). Therefore, the Al abundance in a sample is commonly used to infer the amount of detrital input into the system. Bulk-fraction TM abundances for our samples were plotted against Al content (Figure 11). Trace metals that show a correlation with Al content (TM increases with increasing Al content) are of primarily detrital origin, whereas those that do not, are of primarily non-detrital origin. Mo, Cr, and V, correlate well with Al abundance and are therefore of primarily detrital origin (Figure 11), whereas Cd does not show an increase in abundance with Al, and is not a function of detrital input.

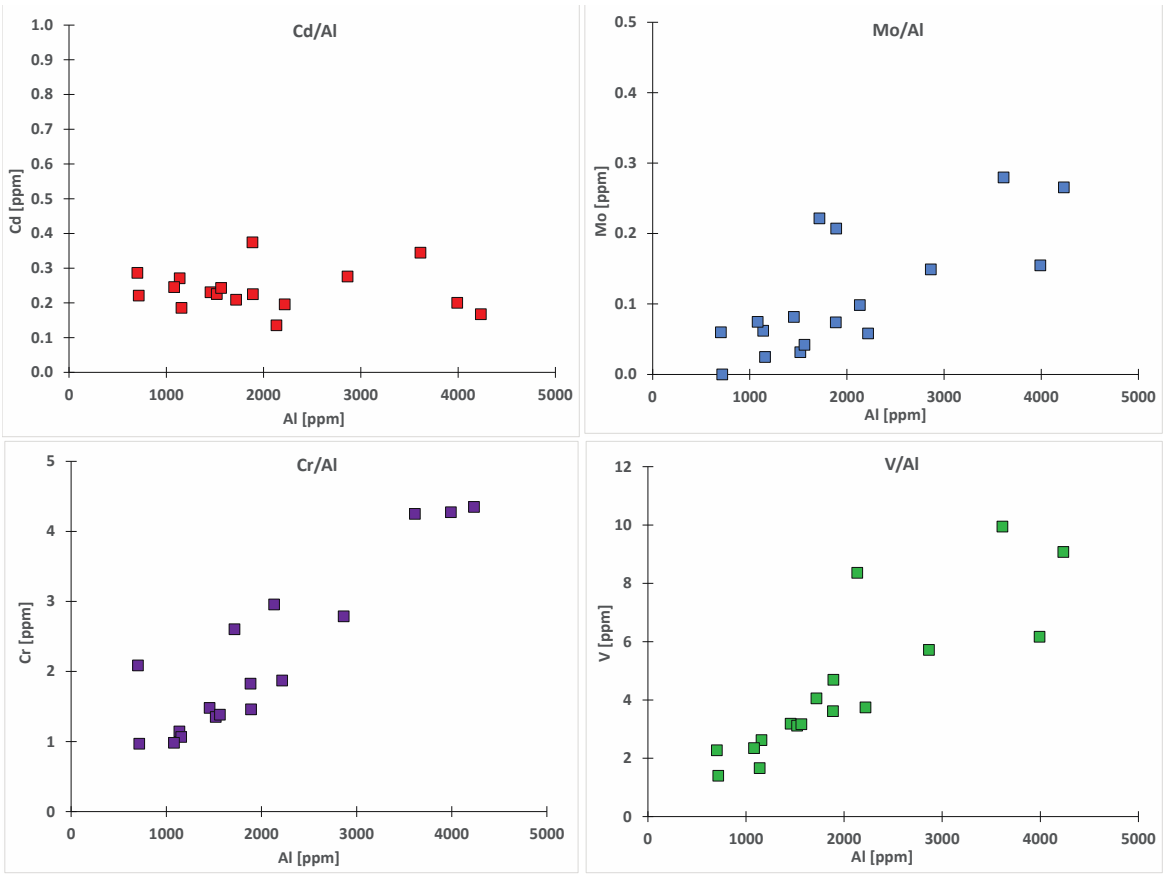

Figure 11: Crossplots of bulk-fraction TM/Al content. Those that correlate well with Al (Mo, Cr, V) are inferred to be of primarily detrital origin, while those that do not show any correlation (Cd) are likely related to processes occurring in the water column.

Through comparison of the bulk-fraction values relative to the carbonate-fraction for each TM, the relative TM content that was sourced from the seawater, and therefore influenced by processes affecting seawater TM abundance, can be determined. For metals with significantly lower carbonate-fraction than the bulk-fraction, it is likely that there was substantial TM input from sources other than seawater including detrital input, or input linked to early diagenetic (biologic) processes occurring below the sediment-water interface. As the difference between the two fractions increase, so does the relative difference in inputs. For TMs where the carbonate-fraction represents a significant portion of the bulk-fraction

TM content, TMs were influenced more by processes effecting the seawater TM content, as opposed to detrital and early diagenetic input into the sediment. These relative bulk-fraction and carbonate-fraction abundances change across the section, indicating a change in either detrital input, early diagenetic processes, or paleoseawater conditions. In the case where bulk-fraction abundance decreases while carbonate-fraction abundance is stable, it is most likely that there was a decrease in detrital input due to a change in sea level or sediment source.

The 'bulk-vs-carbonate' fraction relationship can be used as way to qualitatively assess the relative changes in continent-derived detrital and early diagenetic input compared to the seawater-derived or hydrogenous content for the study outcrop. Bulk-fraction and carbonate-fraction content for Cd and P follow similar trends (Figure 9), providing additional evidence that the Cd content was primarily sourced from the seawater, with little detrital or early diagenetic influence. Similar to Cd, Ba shows little non-seawater derived content, as both bulk-fraction and carbonate-fraction follow the same average of approximately 5 ppm. It should be expected that these TMs reflect seawater abundances and are often used as paleoproductivity proxies (Tribovillard et al.,2006). Vanadium, U, and Cr show bulk fractions that vary relative to carbonate-fractions through time. Samples around 2 m have bulk-fraction abundances that are 600-800% greater than those of the carbonate-fraction. Though from the interval 5.75 to 7 m, the bulk-fractions are only 100-200% greater, increasing as they approach 7 m. Overall, a correlation with Al abundance suggests that V, Cr, and U content is primarily detrital, though the 'bulk-vs.-carbonate' fraction relationship shows changes across the section, and subsequently through time. Titanium bulk-fraction

abundances are consistently 300-400% greater than the carbonate-fraction, indicating a primarily detrital origin, as expected for Ti (Figure 9).

V, U, and Mo, as Paleoredox Proxies

The bulk-fraction data from this study shows that no significant enrichments, relative to average shale (Wedepohl, 1971), occur in V, U, and Mo (average EFs < 4.5). Uranium shows an average depletion with an EF of 0.70. The lack of enrichment in Mo suggests that the environment was not under euxinic conditions during deposition, while the lack of V and U enrichments suggest that anoxic conditions did not exist. While EFs for V are greater than 1, and EFs for Mo are as high as 4.4, they were not high enough to infer significant enrichment. For comparison, sediments that are interpreted to be sporadically anoxic-euxinic in the Namibian upwelling zone have V EFs of 10 while Mo EFs are over 100 (Borchers et al., 2005). The system may have had localized anoxia during short durations of deposition, or possibly abundant sulfide limited to the sediment column, resulting in slightly enriched values in certain samples, though significant overall enrichment is not seen. Therefore, the data from this study indicate that the paleoceanographic system in which these sediments were deposited in was under oxic or possibly suboxic ($2>[O_2]>0.2$ ml/l H_2O) conditions.

To further assess the redox conditions, we plotted Mo/Fe content and compared our samples to samples from modern settings of various redox conditions as presented by Little et al. (2015) (Figure 12). This included samples from both euxinic and oxic systems in Cariaco and the Black Sea, as well as the Peru margin, which is interpreted to be an anoxic to sporadically euxinic environment. The samples from this study fall in the same range as the samples from the oxic Black Sea system. With this comparison, we make the assumption that

the oceanographic processes during the Mississippian were behaving in the same way as they do in modern oceanographic environments. If so, this further supports the conclusion that the Mississippian sediments in the study area were deposited in an overall environment where oxygen was present within the water column (Figure 12). This remains consistent with the paleogeographic interpretation of a distally-steepened ramp that was open to ocean circulation and oxygen input.

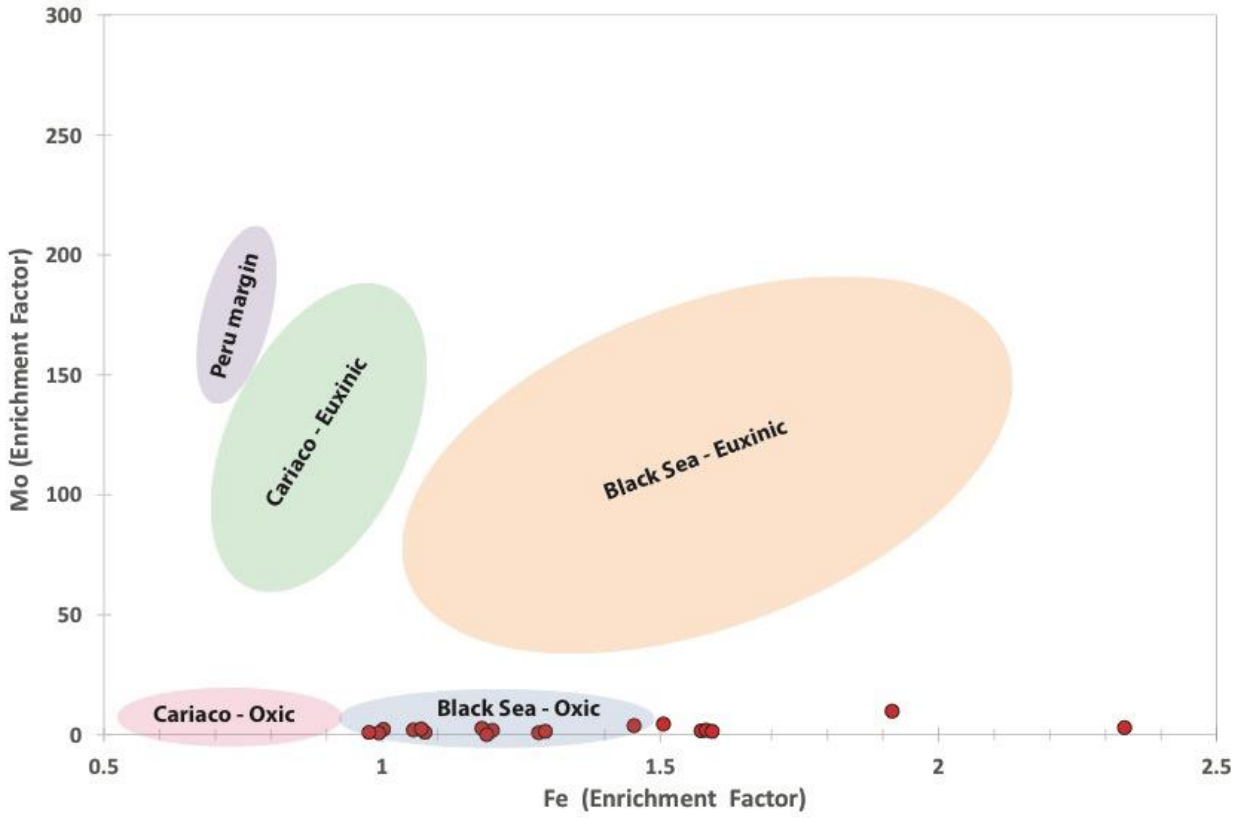

Figure 12: Diagram showing Mo/Fe EF ratios for the samples from this study (red dots), as well as ranges for samples from different environments as presented by Little, et al. (2015). Note that the samples from this study fall within the Black Sea-Oxic range. All EFs are normalized to average shale compositions.

Comparing TM data from carbonate samples to previously published data on organic-rich shales is not straightforward. Comparing the TM values of samples with very different lithology and overall compositions, as well as using average shale values in calculating our enrichment factors leads to uncertainties that cannot be easily quantified. However, at this time there is little TM data for carbonates which we can compare to, and no average carbonate values which we can use to calculate EFs. Therefore, until data is available on a reference composition for the average carbonate, we are limited to the use of average shale compositions when calculating our enrichment factors. We may also correct our calculations for the carbonate dilution, estimating the TM content as if we only had the "shale" fraction. However, with such an approach, our TMs and Al content would scale up proportionally, resulting in the same enrichment factors as discussed.

Chemostratigraphic Potential of TMs

Relative enrichments and depletions in TM abundances of rock units may be used for chemostratigraphic correlation on a local, and possibly regional scale. For the study area, Cd, P, and Ti trends discussed above may provide a way to correlate stratigraphy, though due to the gradual nature of these TM trends, and the relatively low magnitude of change, correlation would be difficult and limited to low-frequency (3^{rd}-order scale) intervals. Titanium may provide higher-frequency cycles, though it would be difficult to distinguish one trend from another, as they do not differ in character or magnitude. Trace metals that show distinct, high magnitude, short-duration enrichments or depletions would be more recognizable and easier to correlate on a regional scale.

It is possible that the TMs measured in this study do vary on higher-frequency or more distinct trends within the outcrop, because our dataset is limited by the sampling resolution. For example, V, U, and Cr bulk-fraction abundances show a single outlier just above 10 m (Figure 9). Unfortunately, there is a lack of data in close stratigraphic proximity to that data point, so it remains unclear whether it is an outlier, or it reflects an actual enrichment in the TM content of the rock. If an enrichment exists, it could be used to correlate that rock unit with other rocks units that may share a similar V, U, and Cr, enrichment. This shows the importance of sampling resolution when attempting to correlate using chemostratigraphy. At best, correlation is only possible on the scale in which data is obtained, and often, as in this case, higher resolution data is needed to determine trends.

The advantage of using TMs for rock characterization and correlation is that each TM offers an additional parameter to use. Different sets of TMs are influenced by different processes and subsequently provide different paleoenvironmental information. Therefore, the specific TMs that may be useful for correlation are dependent on what processes are dominant in the basin at the time of deposition. For example, if changes in redox conditions occur within the interval of interest, variations in Mo, U and V may be seen, and used for correlation. If the water column remains oxic during the entire interval of interest, the above mentioned metals may be of limited use and other metals such as those used as proxies for productivity or detrital input should be examined. The same metals cannot be expected to provide the same correlation potential in different basins, because the processes affecting TM content change along with differing paleoceanographic conditions. Due to this, a single TM enrichment or depletion should not be used for correlation, but rather a set of TM data would

be more effective in reconstructing paleoenvironmental conditions during deposition of the sediments

CHAPTER V

SUMMARY AND CONCLUSIONS

This study assessed the potential of using two geochemical parameters, CAS sulfur isotope compositions, and TM abundances, as novel chemostratigraphic correlation tools in carbonate systems. Each parameter is shown to have certain advantages and disadvantages that must be considered when attempting to use them for correlation. In this study, $\delta^{34}S_{CAS}$ values show trends that may be recognized on 5-10 Ma time scales, though due to the long residence time of sulfur, higher-frequency enrichments/depletions are difficult to recognize when working in open ocean basins. However, $\delta^{34}S_{CAS}$ can be used for low-frequency (>5 Ma time scales) correlation with the global seawater sulfur isotope record. Sulfur isotope compositions may offer enhanced potential for correlation when working in restricted basins, as higher-frequency cycles in $\delta^{34}S_{CAS}$ may be seen due to the smaller sulfate pool. Sulfur isotopes may be affected by diagenetic processes, so a thorough diagenetic investigation for the study area must be completed prior to any correlation application.

The potential of a specific TM for correlation changes from one study area to another depending on the environmental changes that occurred within the system. In this study, Cd, P, and Ti show potential trends that could be used for correlation, although such trends are only evident on 5-10 Ma time-scales (3^{rd}-order sequences). Other metals that are used as paleoredox indicators (V,U, Mo) may prove useful in other locations where environments

underwent rapid fluctuations between oxic, anoxic, and euxinic conditions, resulting in high-amplitude spikes in abundance. These high-amplitude spikes would be more effective at correlating units from one location to another, as they are more recognizable than the low-amplitude trends seen in this study. Variations in TM abundance represent changes in the environmental processes occurring at the time of deposition, therefore, if the system was relatively stable, TMs associated with those processes will not reflect trends that can be used for correlation.

For both $\delta^{34}S_{CAS}$ and TM abundance the sampling resolution of the study was inadequate to fully delineate possible higher frequency trends. Certain TM abundances may change more rapidly across the outcrop than the data show, though they could not be defined due to the sample density. For these and other geochemical tools, the detail at which units can be defined and correlated relies on the resolution for which data is obtained. For example, the characterization and correlation of meter-scale geochemical units necessarily requires sub-meter scale sampling density. Therefore, it is necessary to emphasize the importance of considering sampling resolution prior to any future studies and to adjust sampling according to the goal of the study.

Aside from the possible use as correlation tools, $\delta^{34}S_{CAS}$ and TM data provides valuable paleoceanographic information about the Mississippian carbonate system. The $\delta^{34}S_{CAS}$ values for this study match those of global seawater, indicating the basin was open to global circulation, supporting the current paleogeographic interpretation. Trace metal content, namely, the lack of significant V, U, or Mo enrichments, indicates that deposition of the studied strata occurred under oxic conditions, as opposed to anoxic or euxinic. Ratios for Mo/Fe also fall within the range of those taken from an oxic shelf in a previous study (Little

et al., 2015). The presence of oxygen along the shelf margin suggests ocean circulation, further supporting the interpretation as an open ocean basin.

Further work is necessary to fully assess the potential of both $\delta^{34}S_{CAS}$ and TM abundances as such correlation tools, and if they have advantages over the more commonly used $\delta^{18}O$ and $\delta^{13}C$ isotopes of carbonates. It is clear that CAS sulfur variations through time do not occur with high enough frequency to use for regional correlation in a non-restricted basin, though the potential in a restricted basin is still unclear. If a similar study, though with a high sampling density (10-30 cm intervals) was carried out in a basin that is known to have been significantly restricted during the majority of deposition of the sampled strata, an increase in fluctuation of $\delta^{34}S_{CAS}$ values may be seen.

For both sulfur isotope compositions and TM content, a study based on high-density sampling (< 0.5 m intervals) of drill cores would be very valuable. Core sampling would not only give the opportunity for a more complete stratigraphic interval to be sampled, but it would be closer to simulating the conditions of an industry application, where core material is often more accessible than outcrops. Furthermore, more work on the nature of carbonate associated sulfate and trace metals, and how various diagenetic processes affect them, is necessary to fully understand the associated geochemical systems.

The development of an effective geochemical tool that can be used for regional correlation within heterogeneous systems is of interest to both academic researchers and industry professionals. Being an important hydrocarbon reservoir, a chemostratigraphic method to correlate rocks within the Mississippian limestone in the Midcontinent may prove useful to the hydrocarbon industry. Once refined, geochemical correlation tools tested here

may offer unconventional solutions to the correlation problems associated with conventional lithostratigraphic correlation methods in heterogeneous carbonate reservoirs

REFERENCES

Algeo, T.J., Maynard, J.B., 2004, Trace-element behavior and redox facies in core shales of Upper Pennsylvanian Kansas-type cyclothems: Chem. Geol. V. 206, p. 289-318.

Algeo, T.J., Luo, G.M., Song, H.Y., Lyons, T.W., Canfield, D.E., 2015, Reconstruction of secular variation in seawater sulfate concentrations: Biogeosciences, v. 12, p. 2131-2151.

Algeo, T.J., Rowe, H., 2012, Paleoceanographic applications of trace-metal concentration data: Chemical Geology, v. 324-325, p. 6-18.

Boardman, D.R. II, Thompson, T.L., Godwin, C., Mazzullo, S.J., Wilhite, B.W., Morris, B.T., 2013, High-resolution conodont zonation for Kinderhookian (Middle Tournaisian) and Osagean (Upper Tournaisian-Lower Visean) strata of the Western Edge of the Ozark Plateau, North America: Shale Shaker, p. 98-151.

Borchers, S.L., Schnetger, B., Böning, P., Brumsack, H.-J., 2005, Geochemical signatures of the Namibian diatom belt: Perennial upwelling and intermittent anoxia: Geochemistry, Geophysics, Geosystems, v. 6, no. 6, p. 1-20.

Beer, N.A, Wing, S.R., Hu, Y., 2011, Physical versus biological control of element incorporation into biogenic carbonate: an *in situ* experiment in a New Zealand fjord: Mar. Ecol. Prog. Ser., v. 433, p. 289-301.

Bergersen, E., 2016, Geochemical signatures as a chemostratigraphic tool to correlate stacked carbonates of the Glorieta, Victorio Peak, Cutoff, and Upper San Andres Formations, West Dog Canyon, Guadalupe Mountains, New Mexico: Master's thesis, University of Texas, El Paso, TX, 112 p.

Bernasconi, S.M., Meier, I., Wohlwend, S., Brack, P., Hochuli, P.A., Bläsi, H., Wortmann, U.G., and Ramseyer, K., 2017, An evaporite-based high-resolution sulfur isotope record of Late Permian and Triassic seawater sulfate: Geochimica et Cosmochimica Acta, v. 204, p. 331–349.

Bruland, K.W., Lohan., M.C., 2003, Controls of trace metals in seawater: Treatsie on Geochemistry, v. 6, p 23-47.

Brunner, B., and Bernasconi, S.M., 2005, A revised isotope fractionation model for dissimilatory sulfate reduction in sulfate reducing bacteria: Geochimica et Cosmochimica Acta, v. 69, p. 4759–4771.

Burdett, J.W., Arthur, M.A., Richardson, M., 1989, A Neogene seawater sulfur isotope age curve from calcareous pelagic microfossils: Earth and Planetary Science Letters, v. 94, p. 189-198.

Calvert, S.E, Pederson, T.F., 1993, Geochemistry of recent oxic and anoxic sediments: implications for the geologic record: Marine Geology, v. 113, p. 67-88.

Canfield, D.E., 2001, Isotope fractionation by natural populations, of sulfate-reducing bacteria: Geochimica et Cosmochimica Acta, v. 65, p. 1117-1124.

Canfield, D.E., Farquhar, J., and Zerkle, A.L., 2010, High isotope fractionations during sulfate reduction in a low-sulfate euxinic ocean analog: Geology, v. 38, p. 415–418.

Chen, D., Wang, J., Racki, G., Li, H., Wang, C., Ma, X., Whalen, M.T., 2013, Large Sulphur isotopic perturbations and oceanic changes during the Frasnian-Famennian transition of the Late Devonian: Journal of the Geological Society, London, v. 170, p. 465-476.

Childress, M., 2015, High resolution sequence stratigraphic architecture of a mid-continent Mississippian outcrop in southwest Missouri: Master's thesis, Oklahoma State University, Stillwater, OK, 246 p.

Childress, M., Grammer, G.M., 2015, High resolution sequence stratigraphic architecture of a mid-continent Mississippian outcrop in southwest Missouri: Shale Shaker, p. 206-234.

Claypool, G.E., Holser, W.T., Kaplan, I.R., Sakai, H., Zak, I., 1980, The age curves of sulfur and oxygen isotopes in marine sulfate and their mutual interpretation: Chemical Geology, v. 28, p. 199-260.

Cline, L.M., 1934, Osage formations of southern Ozark region, Missouri, Arkansas, and Oklahoma: AAPG Bulletin, v. 18, no. 9, p. 1132-1159.

Dupont, A.M., (in press), High-Resolution Chemostratigraphy in the "Mississippian Limestone" of North-Central Oklahoma, in G.M. Grammer, J. Gregg, J. Puckette, P. Jaiswal, S., S. Mazzullo, and R. Goldstein (eds), Mississippian Reservoirs of the Mid-Continent, AAPG Memoir 116.

Flügel, E., 2010, Microfacies of carbonate rocks: analysis, interpretation, and application, 2nd Ed.: Springer-Verlag, Berlin, Heidelberg, New York, 1007 p.

Gellatly, A.M., Lyons, T.W., 2005, Trace sulfate in mid-Proterozoic carbonates and the sulfur isotope record of biospheric evolution: Geochimica et Cosmochimica Acta, v. 69, no. 15, p. 3813-3829

Gill, B.C., Lyons, T. W., Saltzman, M.R., 2007, Parallel high-resolution carbon and sulfur isotope records of the evolving Paleozoic marine sulfur reservoir; Palaeoecology, v. 256, p. 156-173.

Gill, B.C., Lyons, T.W., Frank, T.D., 2008, Behavior of carbonate-associated sulfate during meteoric diagenesis and implications for the sulfur isotope paleoproxy, Geochimica et Cosmochimica Acta, v. 72, p. 4699-4711.

Gischler, E., Heindel, K., Birgel, D., Brunner, B., Reitner, J., and Peckmann, J., 2017, Cryptic biostalactites in a submerged karst cave of the Belize Barrier Reef revisited: Pendant bioconstructions cemented by microbial micrite: Palaeogeography, Palaeoclimatology, Palaeoecology, v. 468, p. 34–51.

Guo, Q., Shields, G.A., Liu, C., Strauss, H., Zhu, M., Pi, D., Goldberg, T., Yang, X., 2007, Trace element chemostratigraphy of two Ediacaran-Cambrian successions in South China: implications for organosedimentary metal enrichment and silicification in the early Cambrian: Palaeogeography, Palaeoclimatology, Palaeoecology, v. 254, p. 194-216.

Gutschick, R.C., Sandberg, C.A., 1983, Mississippian continental margins of the conterminous United States: The Society of Economic Paleontologists and Minerologists, No. 33, p. 79-96.

Habicht, K.S., Canfield, D.E., 1997, Sulfur isotope fractionation during bacterial sulfate reduction in organic-rich sediments: Geochimica et Cosmochimica Acta, v. 61, no. 24, p. 5351-5361.

Habicht, K.S., Canfield, D.E., 2001, Isotope fractionation by sulfate-reducing natural populations and the isotopic compositions of sulfide in marine sediments: Geology, v. 29, no. 6, p. 555-558.

Handford, C.R., 1986, Facies and bedding sequences in shelf-storm-deposited carbonates Fayetteville shale and Pitkin Limestone (Mississippian), Arkansas: Journal of sedimentary petrology, v. 56, p. 123-137.

Hastings D.W., Emerson, S.R., Erez, J., Nelson, B.K., 1996, Vanadium in foraminiferal calcite: Evaluation of a method to determine paleo-seawater vanadium concentrations: Geochimica et Cosmochimica Acta, v. 60, p. 3701-3715.

Haq, B.U., Schutter, S.R., 2008, A chronology of Paleozoic sea-level changes: Science, v. 322, p. 64-68.

Hild, E., Brumsack, H.J., 1998, Major and minor element geochemistry of Lower Aptian sediments from the NW German Basin (core Hoheneggelsen KB 40): Cretac. Res. v. 19, p. 615-633.

Kampschulte, A., Strauss, H., 2004. The sulfur isotopic evolution of Phanerozoic seawater based on the analysis of structurally substituted sulfate in carbonates: Chemical Geology, v. 204, p. 255-286.

Kerans, C., Tinker, S.W., 1997, Sequence stratigraphy and characterization of carbonate reservoirs: SEPM, short course notes, no. 40, p. 1-130.

Koch, J., Frank, T., Bulling, T., 2014, Stable-isotope chemostratigraphy as a tool to correlate complex Mississippian marine carbonate facies of the Anadarko Shelf, Oklahoma and Kansas: AAPG Bulletin, v. 98, no. 6, p. 1071-1090.

Lane, H.R., De Keyser, T.L., 1980, Paleogeography of the Late Early Mississippian (Tournaisian 3) in the Central and Southwestern United States: Rocky Mountain Section, SEPM, Paleozoic paleogeography of west-central United States, p. 149-162.

Little, S.H., Vance, D., Lyons, T.W., McManus, J., 2015, Controls on trace metal authigenic enrichment in reducing sediments: insights from modern oxygen-deficient setting: American Journal of Science, v. 315, p. 77-119

Lyons, T.W., Walter, L.M., Gellatly, A.M., Martini, A.M., and Blake, R.E., 2004, Sites of anomalous organic remineralization in the carbonate sediments of South Florida, USA: the sulfur cycle and carbonate-associated sulfate, in Amend, J.P., Edwards K.J., Lyons, T.W (eds.), Sulfur Biogeochemistry – Past and Present: Geol. Soc. Am. Spec. Paper 379, p. 161-176.

Madhavaraju, J., Lee, Y., León, G., 2013, Diagenetic significance of carbon, oxygen, and strontium isotopic compositions in the Aptian-Albian Mural Formation in Cerro Pimas area, northern Sonora, Mexico: Journal of Iberian Geology, v. 39, p. 73-88.

Marenco, P.J., Corsetti, F.A., Kaufman, A.J., Bottjer, D.J., 2008, Environmental and diagenetic variations in carbonate associated sulfate: An investigation of CAS in the lower Triassic of the western USA: Geochimica et Cosmochimica Acta, v. 72, p. 1570-1582.

Mazzullo, S.J., Boardman, D.R., 2013, Revisions of outcrop lithostratigraphic nomenclature in the Lower to Middle Mississippian subsystem (Kinderhookian to basal Meramecian series) along the shelf-edge in southwest Missouri, northwest Arkansas, and northeast Oklahoma: Shale Shaker, p. 414-454.

Mills, J.V., Gomes, M.L., Kristall, B., Sageman, B.B., Jacobson, A.D., Hurtgen. M.T., 2017, Massive volcanism, evaporate deposition, and the chemical evolution of the Early Cretaceous ocean: Geology, v. 45, no. 5, p. 475-478.

Millero, F. J., 2005, Chemical Oceanography, 3rd Ed.: CRC Press, Boca Raton, Florida, 530 p.

Mohammadi, S., Greg, J.M., Shelton, K.L., Appold, M.S., Puckette, J., in press, Influence of late diagenetic fluids on Mississippian carbonate rocks on the Cherokee-Ozark Platform, NE Oklahoma, NW Arkansas, SW Missouri, and SE Kansas, in G.M. Grammer, J. Gregg, J. Puckette, P. Jaiswal, S. Mazzullo, R. Goldstein (eds), Mississippian Reservoirs of the Mid-Continent, AAPG Memoir 116.

Morris, B., Mazzullo, S., White, B., 2013, Diagenesis and isotopic evidence of porosity evolution in reef reservoir-analog facies in outcrops of the St. Joe Group (Kinderhookian to basal Osagean) in SW Missouri and NW Arkansas: Search and Discovery Article #50890 (2013), website accessed March, 2017, http://www.searchanddiscovery.com/documents/2013/50890morris/ndx_morris.pdf.

Oehlert, A.M., Lamb-Wozniak, K.A., Devlin, Q.B., Mackenzie, G.J., Reijmer, J.J., and Swart, P.K., 2012, The stable carbon isotopic composition of organic material in platform derived sediments: Implications for reconstructing the global carbon cycle: Sedimentology, v. 59, p. 319–335.

Paytan, A., Kastner, M., Campbell D., Thiemens, M.H., 1998, Sulfur isotope composition of Cenozoic seawater sulfate: Science v. 282, p. 1459-1462.

Paytan, A., Kastner, M., Campbell D., Thiemens, M.H., 2004, Seawater sulfur isotope flunctuations in the Cretaceous: Science, v. 204, p. 1663-1665.

Paytan, A., Gray, E.T., Ma, Z., Erhardt, A., Faul., Kristina, 2011, Application of sulphur isotopes for stratigraphic correlation: Isotopes in Environmental and Health Studies, p. 1-12.

Poulton, S.W., Canfield, D.E., 2005, Development of a sequential extraction procedure for iron: implications for iron portioning in continentally derived particulates: Chemical Geology, v. 214, p. 209-221.

Ramkumar, M., 2015, Chemostratigraphy: Concepts, Techniques, and Applications: Elsevier, Amsterdam, 538 p.

Rees, C.E.,1973, A steady-state model for Sulphur isotope fractionation in bacterial reduction processes: Geochimica et Cosmochimica Acta, v. 37, p. 1141-1162.

Rees, C.E., 1978, Sulphur isotope measurements using SO_2 and SF_6: Geochimica et Cosmochimica Acta, v. 42 (4), p. 383–389.

Rees, C.E., Jenkins, W.J., Monster, J., 1978, The sulfur isotopic composition of ocean water sulphate: Geochimica et Cosmochimica Acta, v. 42, p. 377-381.

Reeves, R.D., Brooks, R.R., 1978, Trace element analysis of geological material: Chemical analysis vol. 51, John Wiley & Sons, 421 p.

Rennie, V.C.F., Turchyn, A.V., 2014, Controls on the abiotic exchange between aqueous sulfate and water under laboratory conditions: Limnology and Oceanography: Methods, v. 12, p. 166–173, doi: 10.4319/lom.2014.12.166.

Rennie, V.C.F., Turchyn, A.V., 2014; The preservation of $\delta^{34}S_{CAS}$ and $\delta^{18}O_{CAS}$ in carbonate-associated sulfate during marine diagenesis: A 25 Myr test case using marine sediments; Earth and Planetary Science Letters, v. 395, p. 13-23.

Sælen, G., Raiswell, R., Talbot, M.R., Skei, J.M., Bottrell, S.H., 1993, Heavy sedimentary sulfur isotopes as indicators of super-anoxic bottom-water conditions: Geology, v. 21, p. 1091-1094.

Sessions, J.P.S., Opfer, C.L., Scott, R.W., (in press), Isotope chemostratigraphy and sequence stratigraphy of the lower Mississippian St. Joe Group in Northeastern Oklahoma to Southwestern Missouri, in G.M. Grammer, J. Gregg, J. Puckette, P. Jaiswal, S. Mazzullo, R. Goldstein (eds), Mississippian Reservoirs of the Mid-Continent, AAPG Memoir 116.

Sim, M.S., Bosak, T., and Ono, S., 2011, Large sulfur isotope fractionation does not require disproportionation: Science, v. 333, p. 74–77.

Shoeia, O., 2012, High resolution stratigraphy of Lower Mississippian strata near Jane, Missouri: Master's thesis, Oklahoma State University, Stillwater, OK, 69 p.

Staudt, W.J., and Schoonen, M.A.A., 1995, Sulfate Incorporation into Sedimentary Carbonates, *in* Vairavamurthy, M.A. and Schoonen, M.A.A. eds., Geochemical Transformations of Sedimentary Sulfur: Washington DC, American Chemical Society, p. 332–345.

Strauss, H., 1997, The isotopic composition of sedimentary sulfur through time: Palaeogeography, Palaeoclimatology, Palaeoecology, v. 132, p. 97-118.

Takano, B., 1985, Geochemical implications of sulfate in sedimentary carbonates: Chemical Geology, v. 49, p. 393-403.

Tessier, A., Campbell, P.G.C., Bisson, M., 1979, Sequential extraction procedure for the speciation of particulate trace metals: Analytical Chemistry, v. 51, no. 7, p. 844-851.

Theiling, B., Coleman, M., 2015. Refining the extraction methodology of carbonate associated sulfate: Evidence from synthetic and natural carbonate samples: Chemical Geology, v. 411, p. 36-48.

Thode, H.G., Monster, J., Dunford, H.B.,1961, Sulphur isotope geochemistry: Geochimica et Cosmochimica Acta, v. 25, p. 150-174.

Thode, H.G., 1991, Sulphur isotopes in nature and the environment: an overview, in Krouse, H.R., and Grineko, V.A. (eds.), Stable isotopes in the assessment of natural and anthropogenic sulphur in the environment: John Wiley and Sons Ltd, p. 1-26.

Tostevin, R., Turchyn, A.V., Farquhar, J., Johnston, D.T., Eldridge, D.L., Bishop, J.K.B., McIlvin, M., 2014, Multiple sulfur isotope constraints on the modern sulfur cycle: Earth and Planetary Science Letter, v. 396, p. 14-21.

Tribovillard, N., Algeo, T.J., Lyons, T., Riboulleau, A., 2006, Trace metals as paleoredox and paleoproductivity proxies: An update: Chemical Geology, v. 232, p.12-32.

Tyson, R.V., Pearson, T.H., 1991, Modern and ancient continental shelf anoxia: an overview, in Tyson, R.V., Pearson, T.H. (eds.), Modern and Ancient Continental Shelf Anoxia: Geol. Soc. Spec. Publ. v. 58, p. 1-26.

Wendler, I., 2013, A critical evaluation of carbon isotope stratigraphy and biostratigraphic implications for Late Cretaceous global correlation: Earth Science Reviews, v. 126, p. 116–146.

Wotte, T., Shields-Zhou G., Strauss, H., 2012. Carbonate-associated sulfate: Experimental comparisons of common extraction methods and recommendations toward a standard analytical protocol. Chemical Geology, v. 326-327, p. 132-144.

Wedepohl, K.H., 1971. Environmental influences on the chemical composition of shales and clays, in Ahrens, L.H., Press, F., Runcorn, S.K., Urey, H.C. (eds.), Physics and Chemistry of the Earth: Pergamon, Oxford, pp. 305–333.

Wedepohl, K.H., 1991. The composition of the upper Earth's crust and the natural cycles of selected metals, in Merian, E. (ed.), Metals and their Compounds in the Environment: VCH-Verlagsgesellschaft, Weinheim, pp. 3–17.

Wortmann, U.G., Bernasconi, S.M., and Böttcher, M.E., 2001, Hypersulfidic deep biosphere indicates extreme sulfur isotope fractionation during single-step microbial sulfate reduction: Geology, v. 29, p. 647–650.

APPENDICES

Figure 13: Photo of the Secondary outcrop, showing Reeds Spring Fm. and Pierson Fm. contact (red dashed line). Samples were collected within 10-30 cm below the marker bed.

Table 2

Vertical Transects $\delta^{34}S_{CAS}$ and Sulfate Concentrations

Sample Name	Transect #	Stratigraphic Height (m)	Formation	$\delta^{34}S_{CAS}$ ‰	CO_3 (%)	Sulfate Conc. mMol/kg	ppm
	VS2						
VS2-1	2	0.38	Compton	17.54	90	2.47	237
VS2-2	2	1.01	Compton	18.35	91	2.43	233
VS2-3	2	1.55	Compton	20.65	96	2.30	221
HSVS2-4	2	2.10	Compton	21.54	90	0.90	87
HSVS2-5	2	2.38	Compton	21.46	90	1.50	144
HSVS4-15a	2	2.50	Compton	12.40	85	4.70	451
HSVS4-15b	2	2.50	Compton	12.32	85	4.70	451
HSVS4-15c	2	2.50	Compton	12.37	85	4.70	451
HSVS2-6	2	4.10	Compton	23.31	90	1.25	120
HSVS4-2	2	4.35	Northview	22.82	66	4.27	410
VS4-6	2	4.35	Northview	23.85	42	7.28	699
VS2-7a	2	5.02	Northview	21.86	58	3.66	352
VS2-7b	2	5.02	Northview	20.96	58	3.66	352
VS2-7c	2	5.02	Northview	21.37	58	3.66	352
VS4-1	2	5.22	Northview	22.91	40	10.16	976
HSVS4-3	2	5.22	Northview	22.62	66	5.82	559
HSVS2-8	2	5.32	Northview	25.57	58	4.26	409
HSVS4-5	2	5.64	Northview	21.93	50	6.49	624
VS2-9a	2	5.82	Pierson	23.74	93	2.60	250
VS2-9b	2	5.82	Pierson	24.03	93	2.60	250
VS2-9c	2	5.82	Pierson	24.31	93	2.60	250
VS2-10	2	6.50	Pierson	24.08	93	4.73	455
VS2-11	2	7.03	Pierson	24.44	93	3.96	381
HSVS4-8	2	8.14	Pierson	21.29	95	3.70	356
VS4-11	2	8.99	Pierson	16.33	87	2.69	258
VS2-12	2	9.23	Pierson	21.26	93	2.70	259
HSVS4-9	2	9.44	Pierson	18.24	96	2.27	218
VS4-10	2	9.44	Pierson	20.18	97	3.27	314
HSVS4-13	2	9.79	Pierson	17.67	88	4.82	463
HSVS4-12	2	9.99	Pierson	14.16	87	2.72	262
VS2-13	2	10.16	Pierson	17.19	93	3.17	304
VS2-14	2	11.15	Pierson	21.91	93	1.30	125
HSVS4-14	2	11.55	Pierson	18.63	95	2.99	287
VS2-15	2	11.95	Pierson	21.91	93	1.55	149

Continued on next page.

Table 2, continued.

Vertical Transects $\delta^{34}S_{CAS}$ and Sulfate Concentrations

Sample Name	Transect #	Stratigraphic Height (m)	Formation	$\delta^{34}S_{CAS}$ ‰	CO_3 %	Sulfate Conc. mMol/kg	ppm
	VS3						
VS3-01	3	0.63	Compton	25.50	90	1.55	149
VS3-02	3	1.67	Compton	25.15	90	25.22	2423
HSVS3-3	3	4.23	Compton	22.46	88	2.56	245
HSVS3-4	3	6.08	Pierson	20.94	97	3.21	309
HSVS3-4NB	3	6.08	Pierson	20.19	97	3.14	302
HSVS3-5(1)	3	10.08	Pierson	24.37	93	1.19	115
HSVS3-5(2)	3	10.08	Pierson	23.74	97	2.00	192
HSVS3-6	3	11.08	Pierson	23.29	93	1.08	104
	VS23c						
VS23c-1	23c	0.53	Compton	22.97	90	1.62	156
VS-23c-2	23c	1.03	Compton	7.37	90	1.70	164
HSVS23c-3	23c	1.55	Compton	22.20	90	1.77	170
VS23c-4	23c	4.10	Compton	23.37	90	1.22	117
VS23c-5	23c	5.64	Northview	25.83	58	1.98	191
Modern-1	Modern		Bahamas	22.09	99	30.14	2895

Samples beginning with 'HS' are hand samples while the rest are short core samples. Stratigraphic height refers to the height above the Woodford Shale contact in meters. $\delta^{34}S_{CAS}$ values are reported in per mille (‰). Carbonate (CO_3) % was estimated from the mass of carbonate and insoluble material in each sample. Sulfate concentrations were calculated gravimetrically. Samples named VS2 and VS4 are both from transect 2. A modern sample is included for comparison.

Table 3

Lateral Transect $\delta^{34}S_{CAS}$ and Sulfate Concentrations

Sample Name	Position (m)	Formation	$\delta^{34}S_{CAS}$ ‰	CO_3 %	Sulfate Conc. mMol/kg	ppm
HSLS1-5	0	Pierson	12.43	84	2.80	269
LS1-5	0	Pierson	12.09	84	4.15	399
HSLS-16	10	Pierson	18.06	78	5.93	570
HSLS1-4	35	Pierson	13.49	84	2.82	271
LS1-4	35	Pierson	13.20	84	2.54	244
HSLS-15	50	Pierson	16.78	93	4.22	405
HSLS1-3	65	Pierson	19.90	84	2.43	233
LS1-3	65	Pierson	16.13	84	3.56	342
HSLS-12	83	Pierson	16.04	76	6.75	648
LS-12	83	Pierson	21.62	94	10.15	975
HSLS1-2	85	Pierson	13.99	84	3.71	357
HSLS-10	103	Pierson	15.91	81	6.49	624
LS-11	103	Pierson	14.34	85	5.21	500
HSLS-8	105	Pierson	17.40	84	5.35	514
LS1-1a	105	Pierson	13.29	84	3.71	357
LS1-1b	105	Pierson	13.04	84	3.71	357
LS1-1c	105	Pierson	13.13	84	3.71	357
HSLS-9	130	Pierson	19.31	79	6.25	601
HSLS-7	140	Pierson	15.28	80	6.82	655
LS-7	140	Pierson	19.19	92	3.09	297
HSLS-13	160	Pierson	18.61	84	6.11	586
HSLS-14	185	Pierson	13.77	83	5.67	545

Samples beginning with ‘HS’ are hand samples while the rest are short core samples. Stratigraphic height refers to the height above the Woodford Shale contact in meters. $\delta^{34}S_{CAS}$ values are reported in per mille (‰). Carbonate (CO_3) % was estimated from the mass of carbonate and insoluble material in each sample. Sulfate concentrations were calculated gravimetrically. A modern sample is included for comparison.

Table 4

Bulk-Fraction TM Content

Sample Name	Stratigraphic Height (m)	Mg	Al	P	Ti	V	Cr	Mn	Fe	Co	Ni
VS2							ppm				
VS2-3	1.55	7890.95	2133.61	131.91	848.36	8.36	2.96	638.21	1782.15	2.68	6.70
VS2-12	2.20	4749.76	4234.32	88.21	706.30	9.07	4.35	658.01	2253.84	7.10	35.55
VS2-9	5.82	2628.32	1138.66	178.20	882.80	1.66	1.14	601.42	956.63	0.51	2.73
VS4-10	6.50	1563.64	1157.02	48.75	768.22	2.62	1.06	623.49	787.03	3.87	8.97
VS2-10a	6.50	1839.63	1455.53	76.37	806.49	3.18	1.48	453.56	816.21	0.96	4.25
VS2-10b	6.50	1925.06	1520.78	78.78	803.30	3.12	1.35	450.15	802.72	0.93	4.22
VS2-10c	6.50	2052.22	1564.17	85.19	805.48	3.17	1.38	453.92	810.92	0.93	4.21
VS2-11	7.03	1832.42	1886.48	89.17	712.55	3.62	1.83	413.09	1295.46	1.15	9.05
VS2-13	10.16	2329.82	3992.21	59.04	712.14	6.17	4.27	782.55	3377.00	11.92	25.61
VS2-14	11.15	1592.00	1081.57	228.73	776.39	2.35	0.98	424.00	614.55	6.86	9.76
VS2-15	11.95	1513.76	717.28	77.19	795.85	1.40	0.97	499.17	452.48	0.90	4.08
VS3											
VS3-2a	1.67	2475.20	1718.18	141.78	729.25	4.05	2.60	383.44	1373.49	0.77	3.74
VS3-2b	1.67	2988.47	2218.51	182.41	686.29	3.74	1.87	356.34	1268.60	0.67	3.46
HSVS3-4	6.08	4496.19	1890.87	85.24	833.31	4.69	1.46	497.23	1458.56	0.97	8.98
HSVS3-5	10.08	2035.48	2864.96	118.98	777.48	5.71	2.79	477.90	1822.74	0.99	19.53
HSVS3-5 (Std.)	10.08	1369.88	703.00	121.50	317.37	2.27	2.09	404.35	871.31	0.68	13.95
HSVS3-6	11.08	2656.05	3613.53	196.98	1027.68	9.94	4.25	549.47	2262.70	7.03	30.07

Continued on next page.

Table 4, continued.

Sample Name	Stratigraphic Height (m)	Zn	Mo	Cd	Ba	Pb	Th	U
				Bulk-Fraction TM Content				
VS2					ppm			
VS2-3	1.55	15.26	0.10	0.14	5.40	0.70	0.42	0.04
VS2-12	2.20	19.36	0.27	0.17	15.71	1.91	0.73	0.09
VS2-9	5.82	13.76	0.06	0.27	3.65	0.81	0.39	0.03
VS4-10	6.50	11.52	0.02	0.19	6.28	1.14	0.29	0.03
VS2-10a	6.50	13.82	0.08	0.23	5.81	0.85	0.43	0.04
VS2-10b	6.50	13.76	0.03	0.23	5.96	0.82	0.41	0.04
VS2-10c	6.50	13.71	0.04	0.24	6.37	0.84	0.41	0.04
VS2-11	7.03	11.39	0.07	0.37	7.33	0.76	0.36	0.08
VS2-13	10.16	23.69	0.15	0.20	49.52	3.17	0.64	0.05
VS2-14	11.15	16.04	0.07	0.25	4.73	0.80	0.20	0.03
VS2-15	11.95	12.54	0.00	0.22	3.26	0.65	0.17	0.03
VS3								
VS3-2a	1.67	11.41	0.22	0.21	6.63	0.75	0.36	0.05
VS3-2b	1.67	10.80	0.06	0.20	6.68	0.72	0.34	0.04
HSVS3-4	6.08	40.19	0.21	0.23	4.94	0.93	0.54	0.05
HSVS3-5	10.08	17.03	0.15	0.28	12.99	0.79	0.71	0.05
HSVS3-5 (Std.)	10.08	16.90	0.06	0.29	9.99	0.63	0.14	0.06
HSVS3-6	11.08	22.82	0.28	0.34	13.29	1.31	0.73	0.07

Samples labeled ‘HS’ are hand samples while the rest are short core samples. Stratigraphic height refers to the height above the Woodford Shale contact in meters. Values for vertical transects VS2 and VS3 are included and reported in ppm.

Table 5

Carbonate-Fraction TM Content

Sample Name	Stratigraphic Height (m)	Mg	Al	P	Ti	V	Cr	Mn	Fe	Co	Ni
VS2						ppm					
VS2-1	0.38	4543.91	682.03	56.01	171.67	2.01	1.04	359.65	559.14	6.31	7.55
VS2-2	1.01	6123.88	815.81	42.64	208.29	1.65	0.87	503.46	1134.90	0.71	3.46
VS2-3	1.55	3615.57	108.46	20.01	234.46	0.58	0.26	405.25	410.27	1.43	0.80
VS2-5	2.38	4448.51	760.56	24.65	297.63	1.47	0.80	626.84	729.14	0.45	3.73
HSVS2-6a	4.10	2168.33	529.85	33.16	245.08	0.47	0.37	493.15	496.96	0.24	1.79
HSVS2-6b	4.10	2039.56	501.80	30.71	219.67	0.43	0.34	476.98	478.78	0.23	1.68
VS4-6	4.35	1515.06	238.64	18.18	176.62	0.45	0.93	428.57	345.42	2.13	6.79
VS2-7a	5.02	10052.92	1752.86	34.35	233.25	7.58	3.08	756.28	2975.29	2.83	32.84
VS2-7b	5.02	8174.17	1402.46	24.27	187.99	6.17	2.37	628.50	2488.78	2.38	27.71
VS4-1	5.22	4981.40	166.17	33.39	178.48	1.01	0.78	465.72	814.95	10.44	2.17
HSVS2-8	5.32	3379.41	1955.58	36.71	209.88	7.27	4.74	342.24	1454.60	0.84	8.36
VS2-9	5.82	2633.83	213.33	59.31	299.43	0.26	0.22	441.54	363.76	0.22	0.76
VS2-10a	6.50	2128.57	246.91	48.00	289.66	0.48	0.18	410.13	311.96	0.59	1.32
VS2-10b	6.50	2107.36	244.63	51.03	283.89	0.48	0.18	482.62	315.61	0.59	1.31
VS2-11	7.03	2270.52	318.38	37.63	226.16	0.52	0.26	427.79	379.57	0.81	2.30
VS4-7	8.14	2043.89	128.94	44.92	235.33	0.34	0.27	439.96	263.18	4.65	1.16
VS4-11	8.99	1760.20	88.62	37.02	321.61	0.21	0.16	595.62	237.51	0.96	2.78
VS2-12	9.23	4145.47	634.42	33.39	291.90	1.19	0.52	610.42	493.60	1.17	5.03
VS4-10	9.44	1692.06	90.73	26.10	235.56	0.24	0.13	520.07	235.88	1.78	1.21
HSVS2-4	9.95	4505.30	458.16	34.34	275.62	0.93	0.45	420.07	490.03	0.51	3.22
VS2-13	10.16	2246.62	556.32	28.06	216.16	0.57	0.43	523.17	309.46	4.44	6.51
VS2-14a	11.15	2176.26	234.74	57.13	300.93	0.49	0.26	456.25	244.50	6.06	4.22
VS2-14b	11.15	1787.29	186.36	45.69	277.12	0.34	0.17	506.90	179.36	4.55	3.16
VS2-15	11.95	1663.86	138.41	34.86	298.71	0.26	0.17	407.59	168.31	0.36	0.88

Continued on next page.

Table 5, continued.

Carbonate-Fraction TM Content

Sample Name	Stratigraphic Height (m)	Zn	Mo	Cd	Ba	Pb	Th	U
VS2					ppm			
VS2-1	0.38	8.30	0.00	0.25	3.79	0.99	0.37	0.03
VS2-2	1.01	3.89	0.00	0.13	4.73	0.44	0.30	0.02
VS2-3	1.55	2.14	0.00	0.10	1.15	0.41	0.13	0.01
VS2-5	2.38	3.06	0.00	0.09	5.48	0.44	0.29	0.01
HSVS2-6a	4.10	7.46	0.00	0.09	4.92	0.64	0.29	0.01
HSVS2-6b	4.10	7.09	0.00	0.09	4.82	0.62	0.29	0.01
VS4-6	4.35	3.18	0.00	0.10	10.79	0.56	0.81	0.04
VS2-7a	5.02	7.23	0.00	0.17	8.35	0.97	0.66	0.03
VS2-7b	5.02	6.25	0.00	0.17	7.67	0.90	0.62	0.03
VS4-1	5.22	3.00	0.00	0.12	2.01	0.58	0.50	0.01
HSVS2-8	5.32	6.56	0.00	0.22	13.01	1.26	0.98	0.03
VS2-9	5.82	0.88	0.00	0.20	2.20	0.53	0.20	0.01
VS2-10a	6.50	3.16	0.00	0.20	2.01	0.56	0.21	0.01
VS2-10b	6.50	3.20	0.00	0.19	2.07	0.57	0.22	0.01
VS2-11	7.03	4.00	0.00	0.41	2.23	0.59	0.17	0.03
VS4-7	8.14	20.79	0.00	0.18	2.43	0.82	0.22	0.01
VS4-11	8.99	2.92	0.00	0.16	2.13	0.74	0.21	0.02
VS2-12	9.23	2.16	0.00	0.17	4.55	0.90	0.25	0.02
VS4-10	9.44	1.99	0.00	0.15	2.47	0.70	0.16	0.01
HSVS2-4	9.95	3.13	0.00	0.10	2.93	0.38	0.12	0.01
VS2-13	10.16	5.52	0.00	0.17	22.41	1.13	0.32	0.01
VS2-14a	11.15	2.77	0.00	0.25	2.81	0.47	0.08	0.02
VS2-14b	11.15	1.89	0.00	0.20	2.24	0.39	0.06	0.01
VS2-15	11.95	2.59	0.00	0.18	1.78	0.38	0.10	0.01

Samples beginning with ‘HS’ are hand samples while the rest are short core samples. Stratigraphic height refers to the height above the Woodford Shale contact in meters. Values for vertical transects VS2 and VS3 are included and reported in ppm.

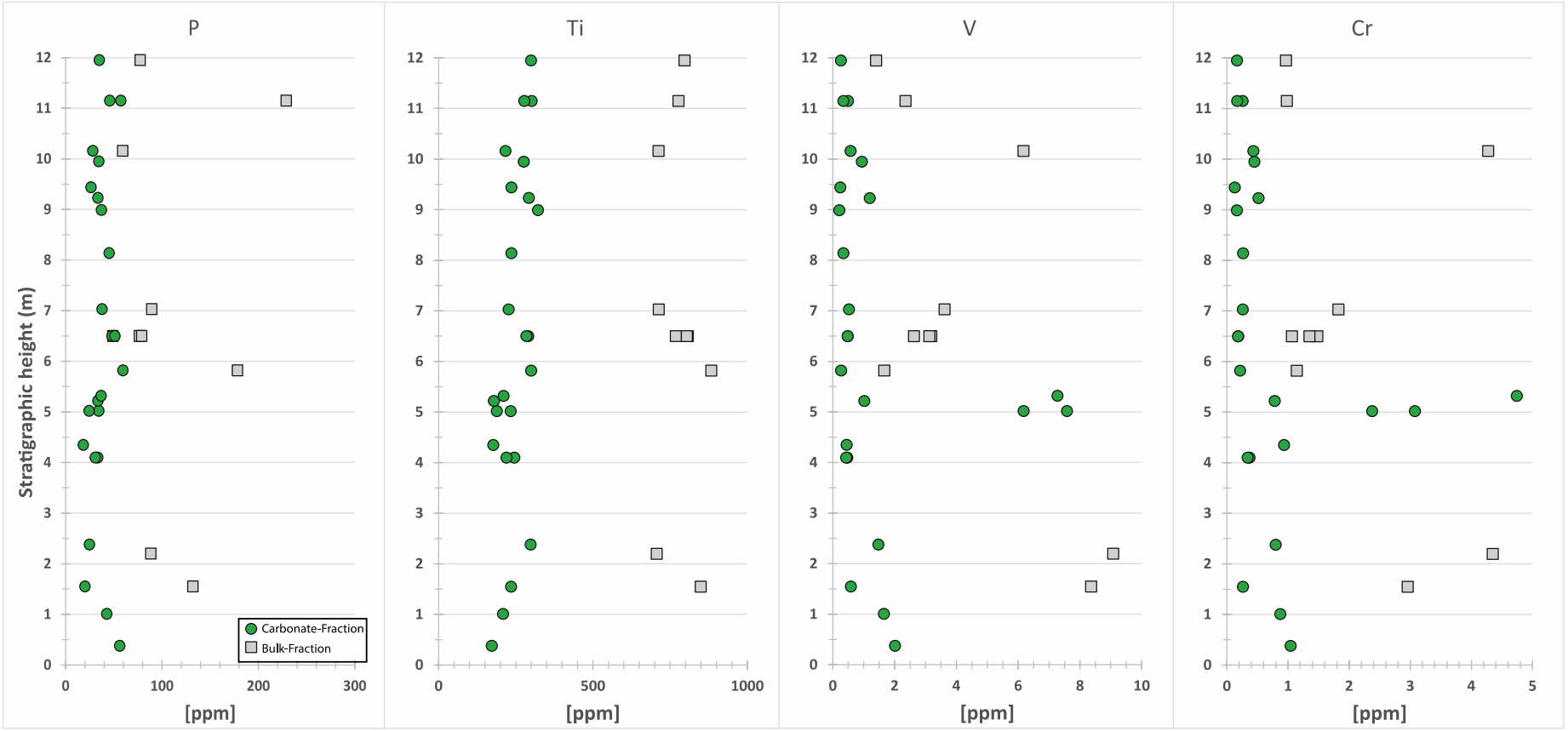

Figure 14: P, Ti, V, and Cr content for VS2. Green circles are carbonate-fraction while gray squares are bulk-fraction. Concentrations are in ppm, and height is in meters above Woodford Shale contact.

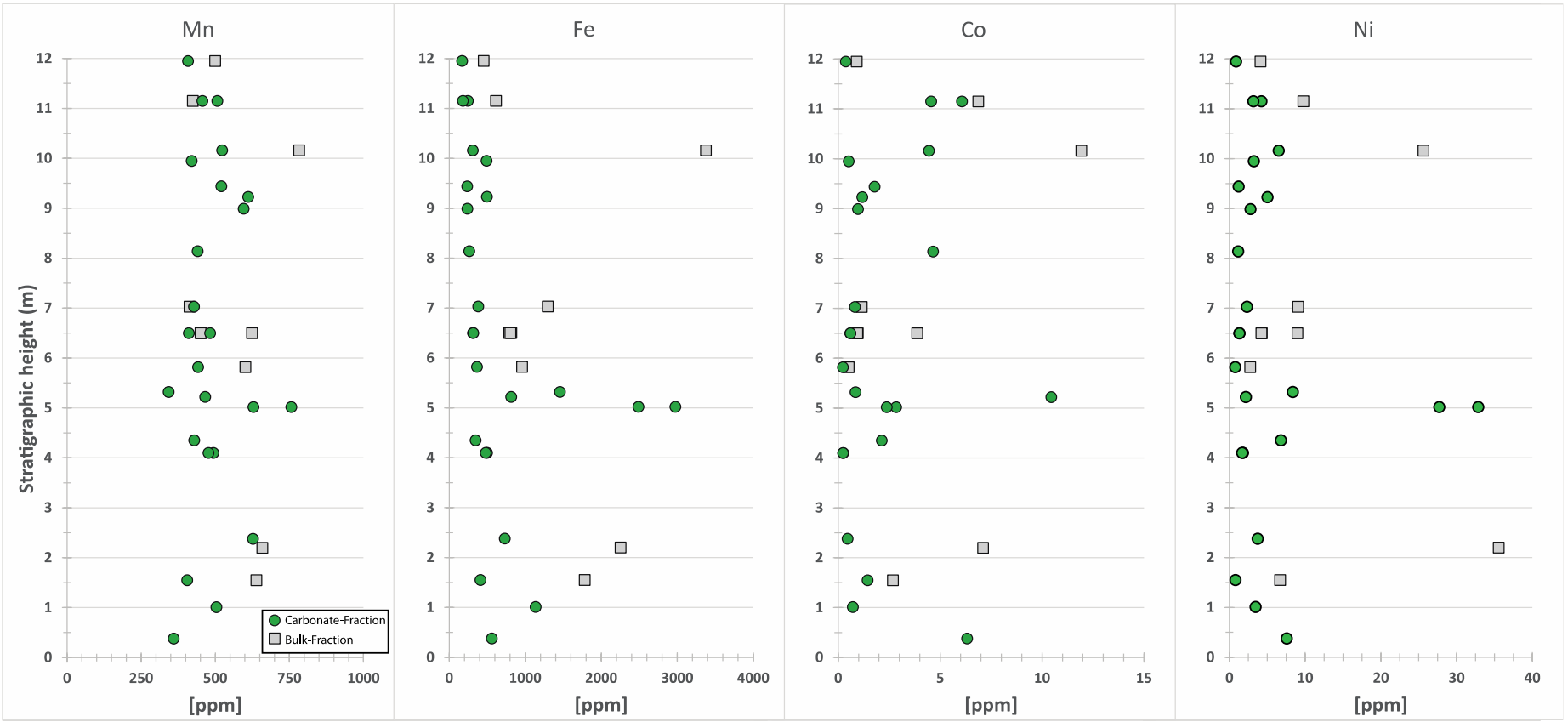

Figure 15: Mn, Fe, Co, and Ni content for VS2. Green circles are carbonate-fraction while gray squares are bulk-fraction. Concentrations are in ppm, and height is in meters above Woodford Shale contact.

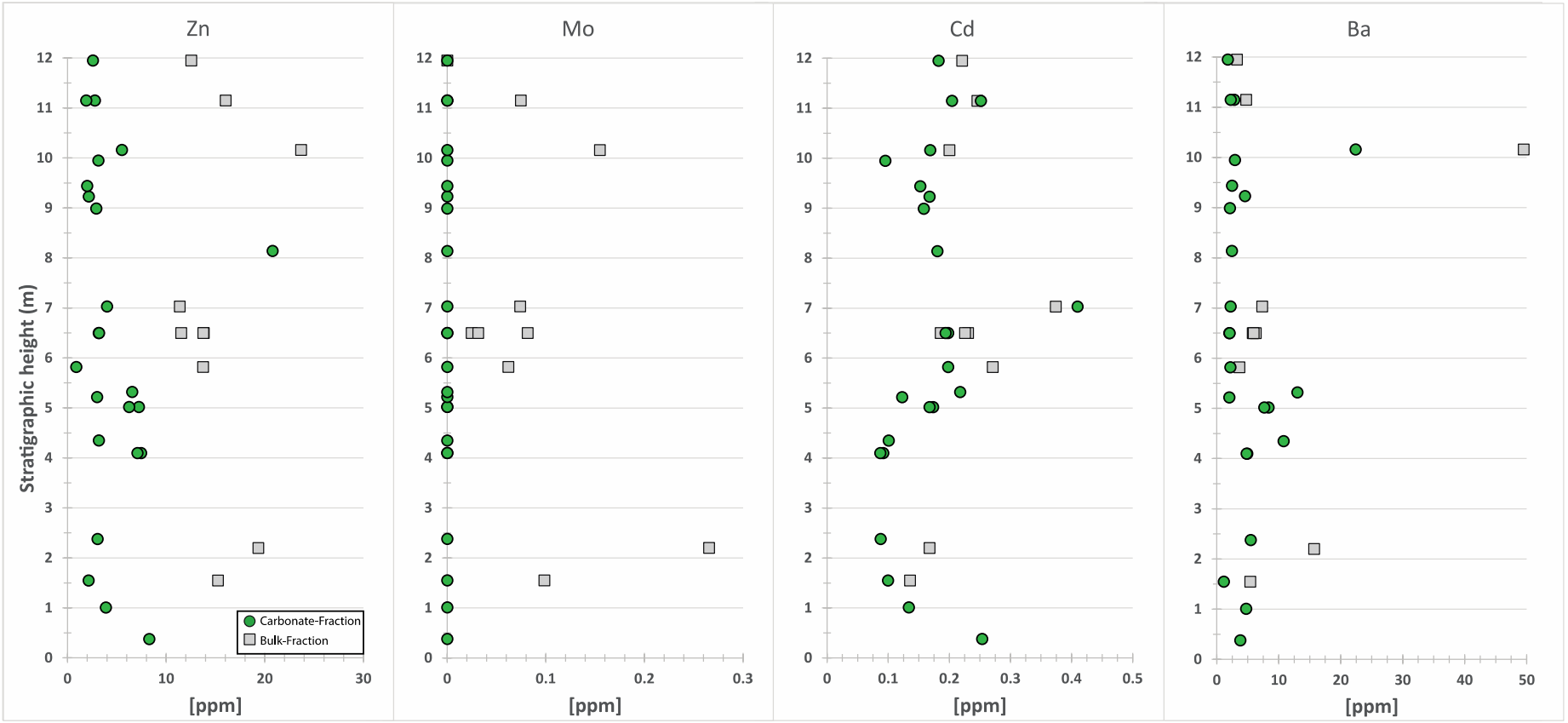

Figure 16: Zn, Mo, Cd and Ba content for VS2. Green circles are carbonate-fraction while gray squares are bulk-fraction. Concentrations are in ppm, and height is in meters above Woodford Shale contact.

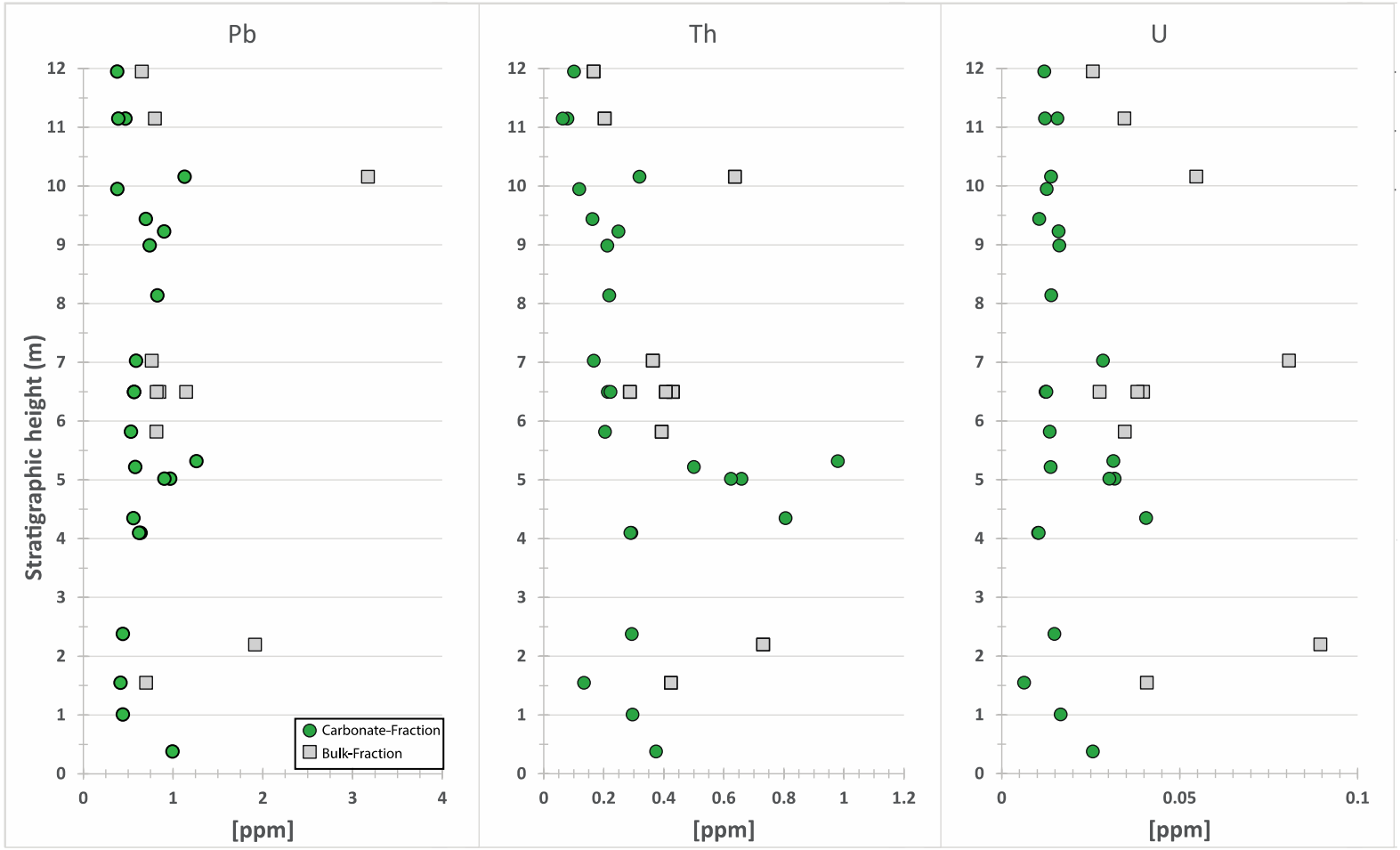

Figure 17: Pb, Th, and U content for VS2. Green circles are carbonate-fraction while gray squares are bulk-fraction. Concentrations are in ppm, and height is in meters above Woodford Shale contact.

Table 6

Bulk-Fraction TM Enrichment Factors

Sample Name	Stratigraphic Height (m)	P	Ti	V	Cr	Mn	Fe	Co	Ni
VS2					Enrichment Factor				
VS2-3	1.55	7.85	7.68	2.68	1.37	31.28	1.57	5.87	4.10
VS2-12	2.20	2.65	3.22	1.47	1.01	16.25	1.00	7.84	10.98
VS2-9	5.82	19.88	14.98	1.00	0.99	55.24	1.58	2.10	3.13
VS4-10	6.50	5.35	12.83	1.55	0.91	56.36	1.28	15.65	10.14
VS2-10a	6.50	6.66	10.71	1.50	1.00	32.59	1.06	3.07	3.82
VS2-10b	6.50	6.58	10.21	1.40	0.88	30.96	0.99	2.87	3.63
VS2-10c	6.50	6.92	9.95	1.38	0.87	30.35	0.98	2.79	3.52
VS2-11	7.03	6.00	7.30	1.31	0.96	22.90	1.29	2.86	6.27
VS2-13	10.16	1.88	3.45	1.06	1.06	20.50	1.59	13.97	8.39
VS2-14	11.15	26.86	13.87	1.48	0.90	41.00	1.07	29.68	11.80
VS2-15	11.95	13.67	21.44	1.33	1.33	72.78	1.19	5.89	7.44
VS3									
VS3-2a	1.67	10.48	8.20	1.61	1.50	23.34	1.51	2.10	2.85
VS3-2b	1.67	10.44	5.98	1.15	0.83	16.80	1.08	1.42	2.04
HSVS3-4	6.08	5.73	8.52	1.70	0.76	27.50	1.45	2.39	6.21
HSVS3-5	10.08	5.27	5.24	1.36	0.96	17.45	1.20	1.62	8.91
HSVS3-5 (Std.)	10.08	21.95	8.72	2.21	2.93	60.16	2.33	4.50	25.93
HSVS3-6	11.08	6.92	5.50	1.88	1.16	15.90	1.18	9.11	10.88
Minimum		1.88	3.22	1.00	0.76	15.90	0.98	1.42	2.04
Maximum		26.86	21.44	2.68	2.93	72.78	2.33	29.68	25.93
Average		9.71	9.28	1.53	1.14	33.61	1.32	6.69	7.65
Average Shale Conc. [ppm]		700	4600	130	90	850	47200	19	68

Continued on next page.

Table 6, continued

Bulk-Fraction TM Enrichment Factors

Sample Name	Stratigraphic Height (m)	Zn	Mo	Cd	Ba	Pb	Th	U
VS2				Enrichment Factor				
VS2-3	1.55	6.69	1.58	43.44	0.39	1.45	1.47	0.46
VS2-12	2.20	4.28	2.14	27.06	0.57	2.01	1.28	0.51
VS2-9	5.82	11.31	1.86	162.73	0.49	3.18	2.55	0.73
VS4-10	6.50	9.32	0.73	109.67	0.83	4.39	1.83	0.57
VS2-10a	6.50	8.88	1.91	108.36	0.61	2.58	2.19	0.65
VS2-10b	6.50	8.47	0.71	101.40	0.60	2.38	1.98	0.60
VS2-10c	6.50	8.20	0.92	106.26	0.62	2.38	1.95	0.61
VS2-11	7.03	5.65	1.34	135.63	0.60	1.80	1.43	1.03
VS2-13	10.16	5.55	1.33	34.28	1.90	3.53	1.18	0.33
VS2-14	11.15	13.88	2.36	155.32	0.67	3.28	1.39	0.76
VS2-15	11.95	16.36	0.00	210.57	0.70	4.05	1.71	0.86
VS3								
VS3-2a	1.67	6.21	4.41	83.15	0.59	1.93	1.54	0.75
VS3-2b	1.67	4.55	0.89	60.30	0.46	1.45	1.14	0.39
HSVS3-4	6.08	19.89	3.74	81.41	0.40	2.18	2.12	0.57
HSVS3-5	10.08	5.56	1.78	65.85	0.69	1.22	1.83	0.40
HSVS3-5 (Std.)	10.08	22.50	2.90	278.72	2.18	4.01	1.46	2.19
HSVS3-6	11.08	5.91	2.65	65.21	0.56	1.61	1.49	0.45
Minimum		4.28	0.00	27.06	0.39	1.22	1.14	0.33
Maximum		22.50	4.41	278.72	2.18	4.39	2.55	2.19
Average		9.60	1.84	107.61	0.76	2.56	1.68	0.70
Average Shale Conc. [ppm]		95	2.6	0.13	580	20	12	3.7

Samples beginning with 'HS' are hand samples while the rest are short core samples. Stratigraphic height refers to the height above the Woodford Shale contact in meters. Enrichment factors were calculated relative to average shale values (ppm) from Wedepohl, 1971, 1991).

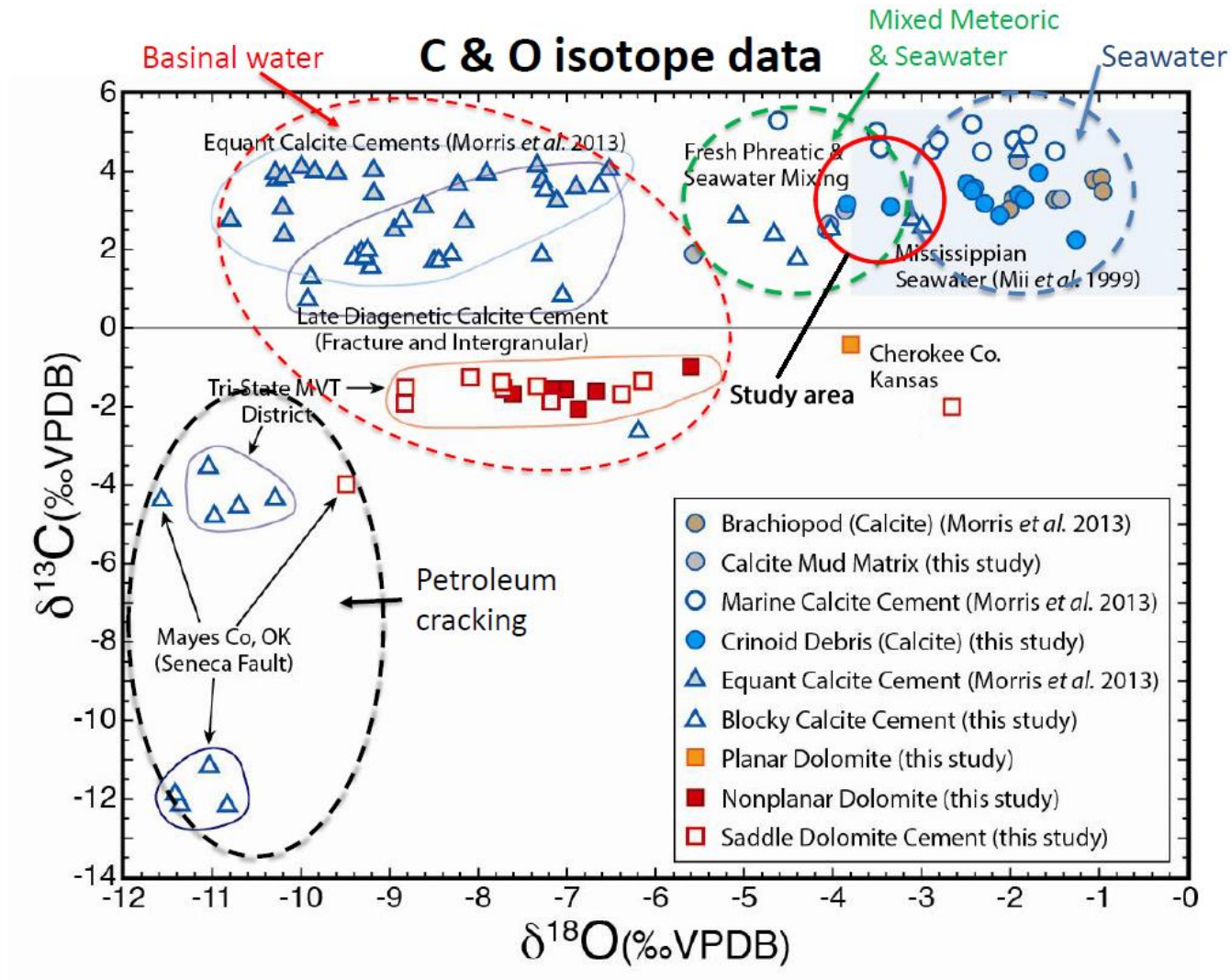

Figure 18: Crossplot of $\delta^{13}C$/ $\delta^{18}O$ values relative to Vienna Pee Dee Belemnite (modified from Mohammadi et al., 2017). Values for the Primary outcrop as reported by Sessions (in press) fall within the red circle.

VITA

Justin W. Steinmann

Candidate for the Degree of

Master of Science

Thesis: ASSESSING THE POTENTIAL OF SULFUR ISOTOPES AND TRACE METALS AS CHEMOSTRATIGRAPHIC CORRELATION TOOLS IN THE "MISSISSIPPIAN LIMESTONE" OF THE MIDCONTINENT

Major Field: Geology

Biographical:

Education:

Completed the requirements for the Master of Science in Geology at Oklahoma State University, Stillwater, Oklahoma in July, 2017.

Completed the requirements for the Bachelor of Science in Earth Science at University of California at Santa Barbara, Santa Barbara, CA/USA in 2015.

Experience:

Field Geologist, UCSB, CA, Earth Science Research Institute, 2014
Teaching Assistant, OSU, OK, 2015-2017
Research Assistant, OSU, OK, 2015-2017
Field Trip Assistant, OSU, OK, 2015-2017

Professional Memberships:

American Association of Petroleum Geologists
Geological Society of America
Oklahoma City Geological Society